The Abdus Salam International Centre for Theoretical Physics

2369-6

CIMPA/ICTP Geometric Structures and Theory of Control

1 - 12 October 2012

Spherical Tokamaks: Achievements and Prospects

Michael Bell

Princeton University
USA

<u>Spherical Tokamaks:</u>
<u>Achievements and Prospects</u>

Michael Bell

former Head of NSTX Experimental Research Operations

Princeton Plasma Physics Laboratory

Princeton University

presented to the

Joint ICTP-IAEA College on Plasma Physics

International Center for Theoretical Physics, Trieste

October 2012

Topics

- Genesis and unique features of the “Spherical Torus” concept
- The worldwide complement of STs and future developments
- ST stability and the effects of non-axisymmetric magnetic fields
- Mitigating divertor heat fluxes
- Controlling plasma-wall interactions through lithium coating
- General features of transport in ST plasmas
- Turbulence measurements and their relationship to transport
- Fast-ion confinement and the effects of MHD instabilities
- Non-inductive generation and sustainment of plasma current

"Spherical Torus" (ST) Pushes the Tokamak to Extreme Toroidicity

- Motivated by potential for increased β *[Peng & Strickler, 1980s]*

$$\beta_{max} \;(= 2\mu_0\langle p\rangle/B_T^2) \;=\; C\cdot I_p/aB_T \;\propto\; C\cdot\kappa/\mathbf{A}q$$

B_T: toroidal magnetic field on axis;
$\langle p\rangle$: average plasma pressure;
I_p: plasma current;
a: minor radius;
κ: elongation of cross-section;
A: aspect ratio (= R/a);
q: MHD "safety factor" (> 2)
C: Constant ~3%·m·T/MA
[Troyon, Sykes - early 1980s]

- Confirmed by experiments
  - **β_{max} ≈ 40%**
    [START (UK) 1990s]

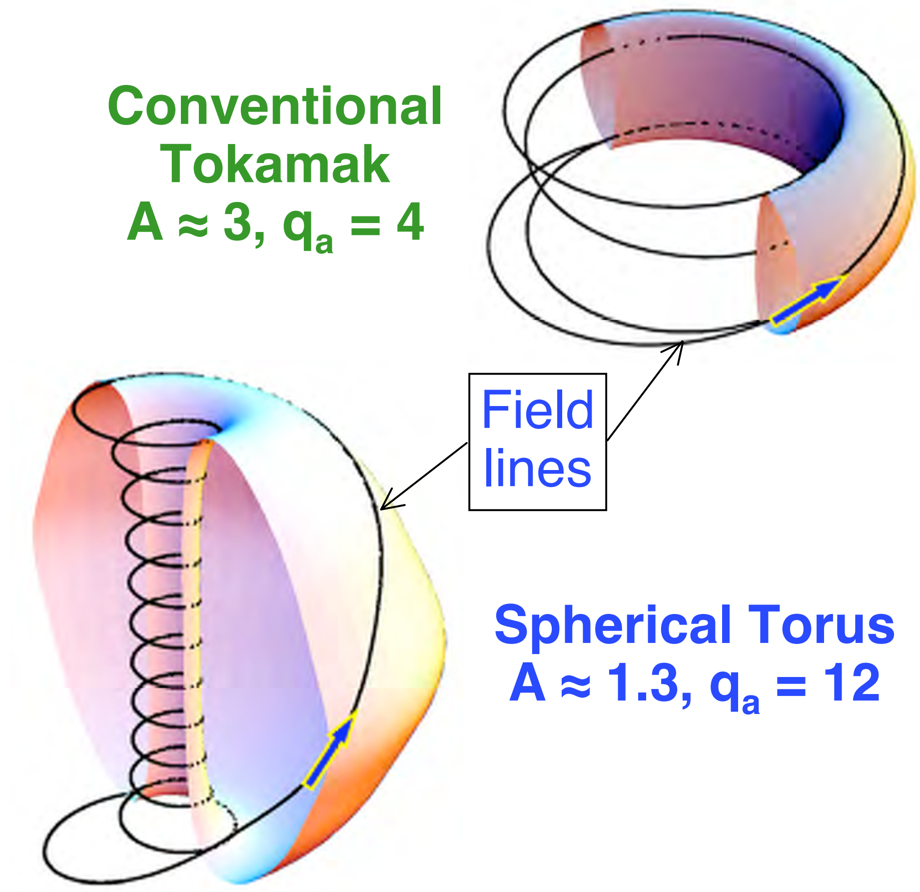

Y-K.M.. Peng et al., *NF* ***26*** *(1986) 769;*
F. Troyon, et al., *PPCF* ***26****, 209 (1984); A. Sykes* et al. *NF* ***39*** *(1997) B247*

Growing Number of STs Now Operating Around the World

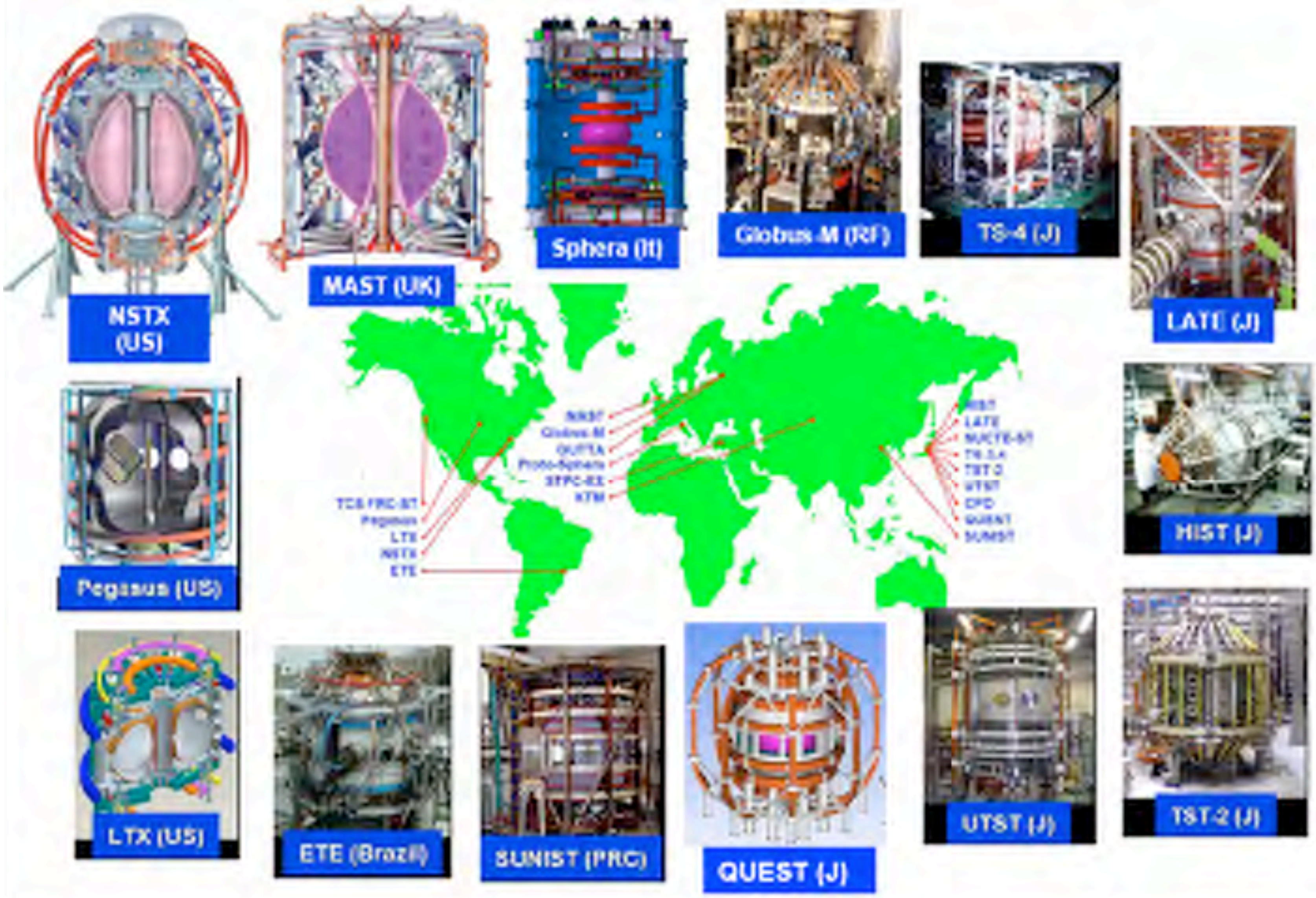

Spherical Torus Complements and Extends Conventional Aspect-ratio Tokamaks

- High β: β_T up to 40%; on axis $\beta \sim 1$
- Extreme cross-section shaping: elongation $\kappa > 2$, $B_P/B_T \sim 1$
- Large fraction of trapped particles: $\sim \sqrt{\varepsilon}$ ($\varepsilon = r/R$)
- Large gyro-radius compared to system size: $\rho_i/a \sim 0.02 – 0.03$
- Large bootstrap current: $I_{Bootstrap} / I_{tot} \sim \sqrt{\varepsilon}\beta_P > 50\%$
  - Affects long-term stability of high-beta plasmas
- Large plasma flow & flow shear: Mach number M ~ 0.5
  - Expect strong effect on ion turbulence
- Large population of supra-Alfvénic fast ions: $v_{NBI}/v_A \sim 4$
  - Mimics alpha-particle population in a burning plasma
- High plasma density at low magnetic field affects electromagnetic waves used for plasma heating

ST Experiments are being Proposed for Fusion Energy Development

- ST combines several potential advantages
  - Compact size
  - High neutron wall loading for nuclear component testing
  - Simplified maintenance scheme
- Considerations for achieving required performance:
  - Adequate confinement

$$\tau_E \propto H I_p$$

  - High bootstrap current fraction

$$f_{BS} \propto q \beta_N$$

  - Adequate margin on safety factor

$$q \propto \left(1 + \kappa^2\right)$$

ST Design Studies

Fusion Nuclear Science Facility

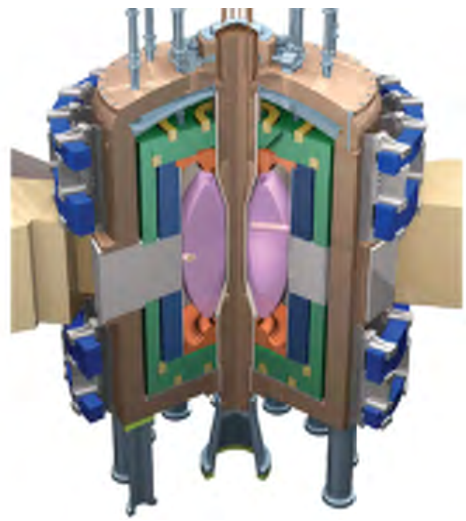

Pilot Power Plant

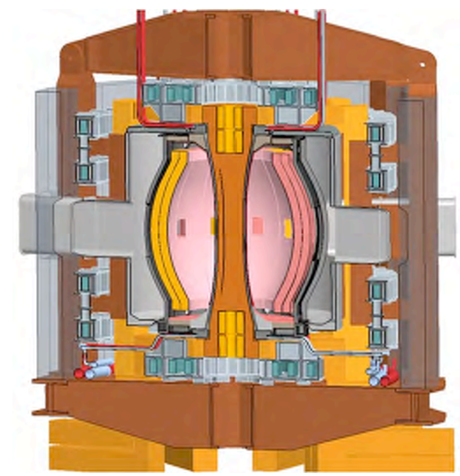

	β_N	κ	$H_{98y,2}$
FNSF	**3-5**	**2.5-3.2**	**1.2-1.6**
Power Plant	**6-8**	**3-3.5**	**1.3-1.6**

NSTX at PPPL Designed to Study High-Temperature Toroidal Plasmas at Low Aspect-Ratio

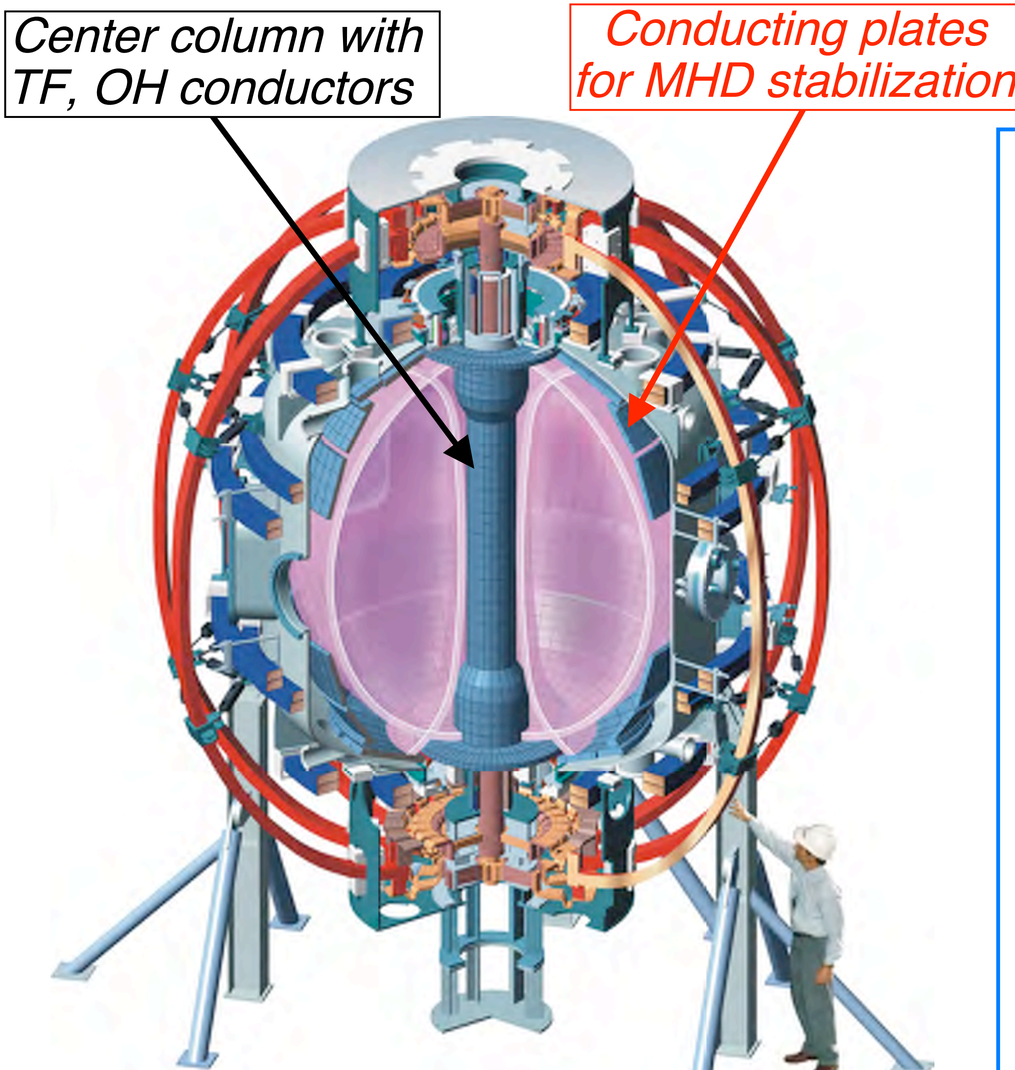

Aspect ratio A	1.27
Elongation κ	2.7
Triangularity δ	0.8
Major radius R_0	0.85m
Plasma Current I_p	1.5MA
Toroidal Field B_{T0}	0.6 T
Pulse Length	1.7s
Auxiliary heating:	
NBI (100kV)	7 MW
RF (30MHz)	6 MW
Central temperature	1 – 3 keV

NSTX *High-Harmonic Fast Wave* System Provides Auxiliary Power for Heating and Current Drive

- 12-element antenna for 6MW coupled power at 30MHz
  - $\omega_{RF} = 10 – 15 \times \omega_{c,D}$ (majority-ion cyclotron frequency)
  - Phase control of currents in antenna elements changes phase velocity of waves launched into plasma
  - $\mathbf{k}_{tor} = \pm(4 – 14)\ m^{-1}$

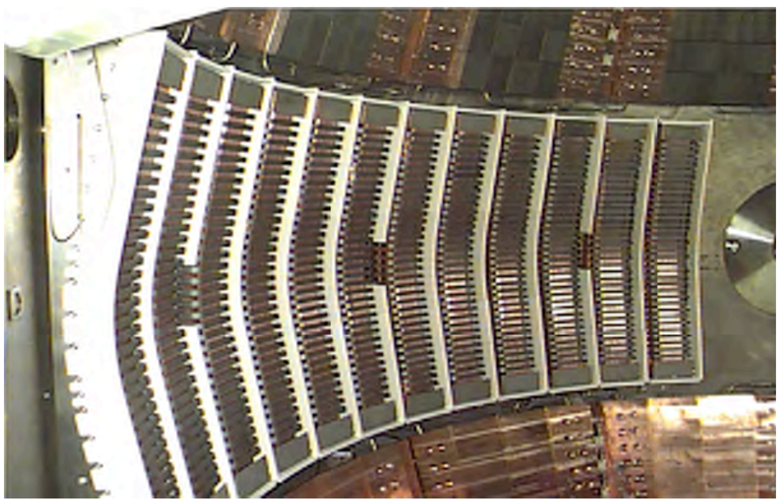

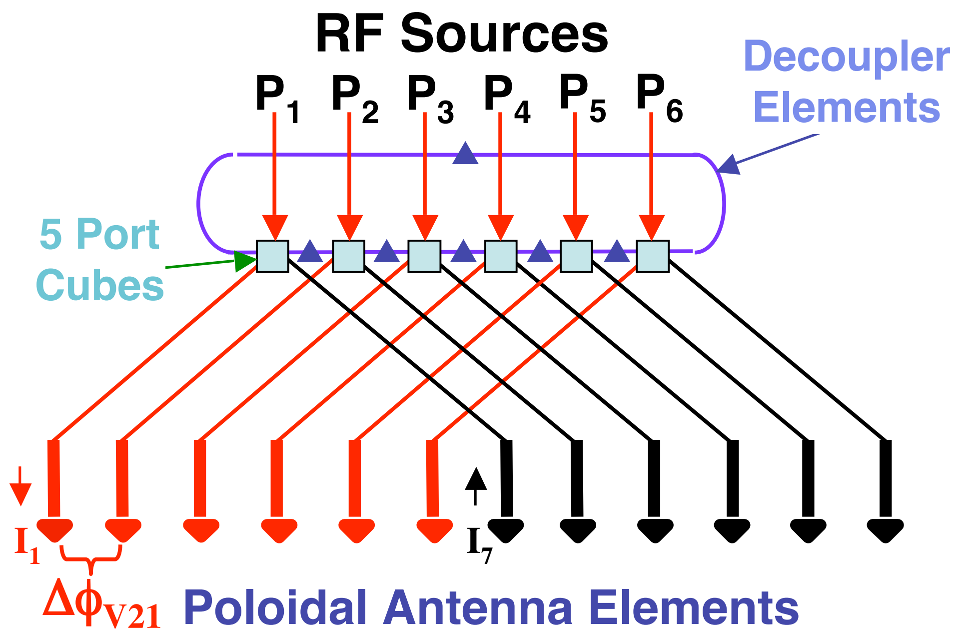

- HHFWs heat electrons by
  - Landau damping: phase velocity $v_{ph} = \omega/k \sim v_{th,e}$
  - Transit-time magnetic pumping: bounce frequency $\varepsilon^{1/2}v_{th,e}/qR \sim \omega_{RF}$

J. Wilson et al., *PoP* **10** (2003) 1733

NSTX Confirmed Capability of ST for High-β in Well-Diagnosed Plasmas

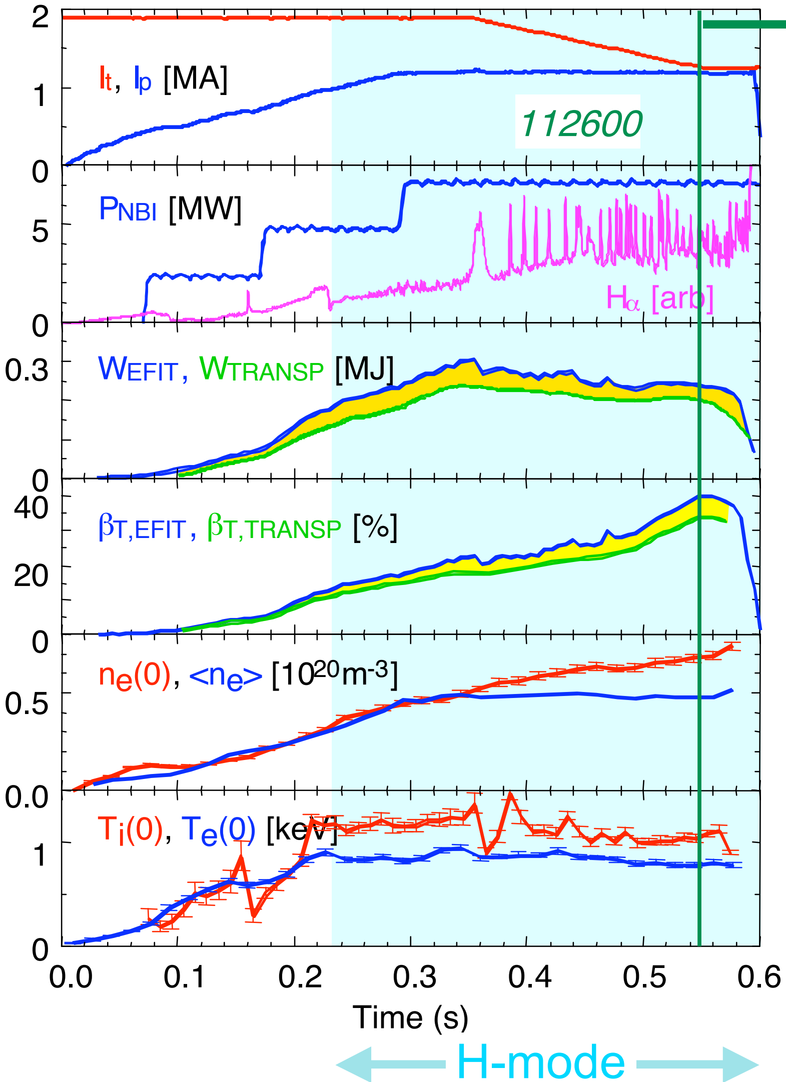

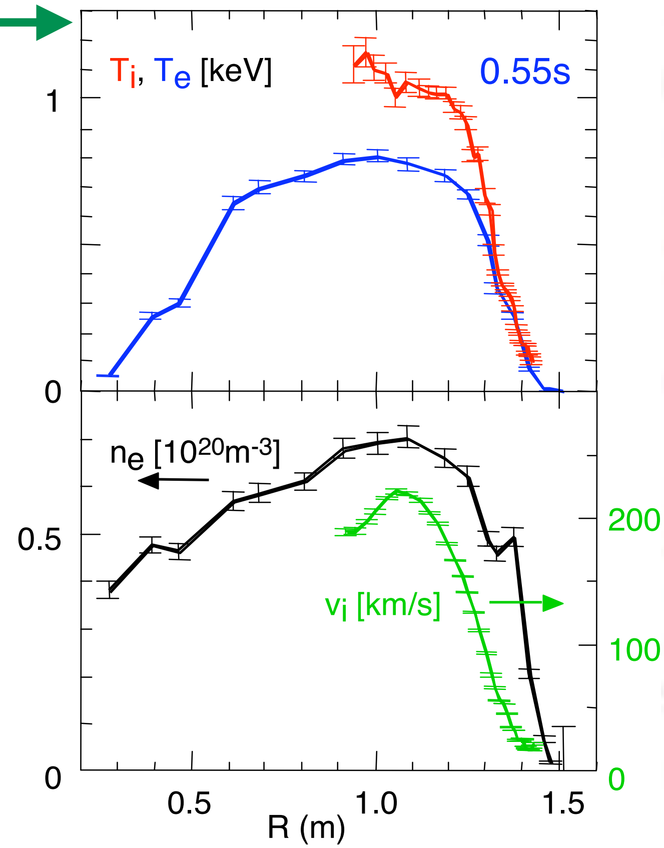

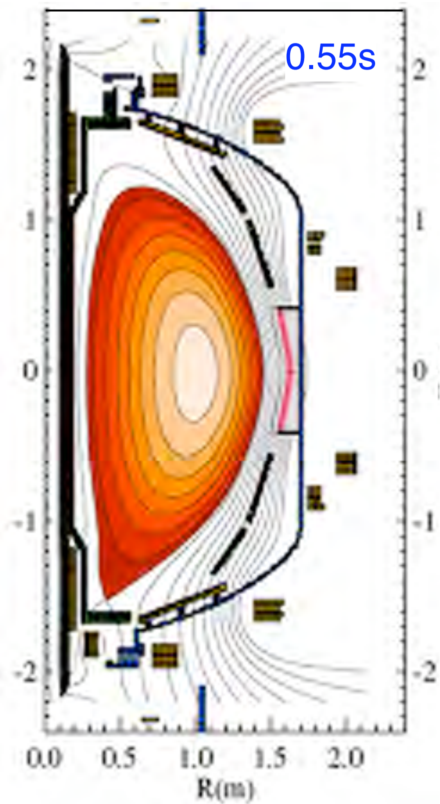

- β_T ($= 2\mu_0\langle p\rangle/B_{T0}^2$) = 38% from magnetic analysis, 34% kinetic
- Achieving high-β facilitated by **broad pressure profile** in H-mode

*J. Menard, et al., Nucl. Fusion **45** (2005) 539*

ST Significantly Exceeds Conventional Tokamak Stability Boundaries

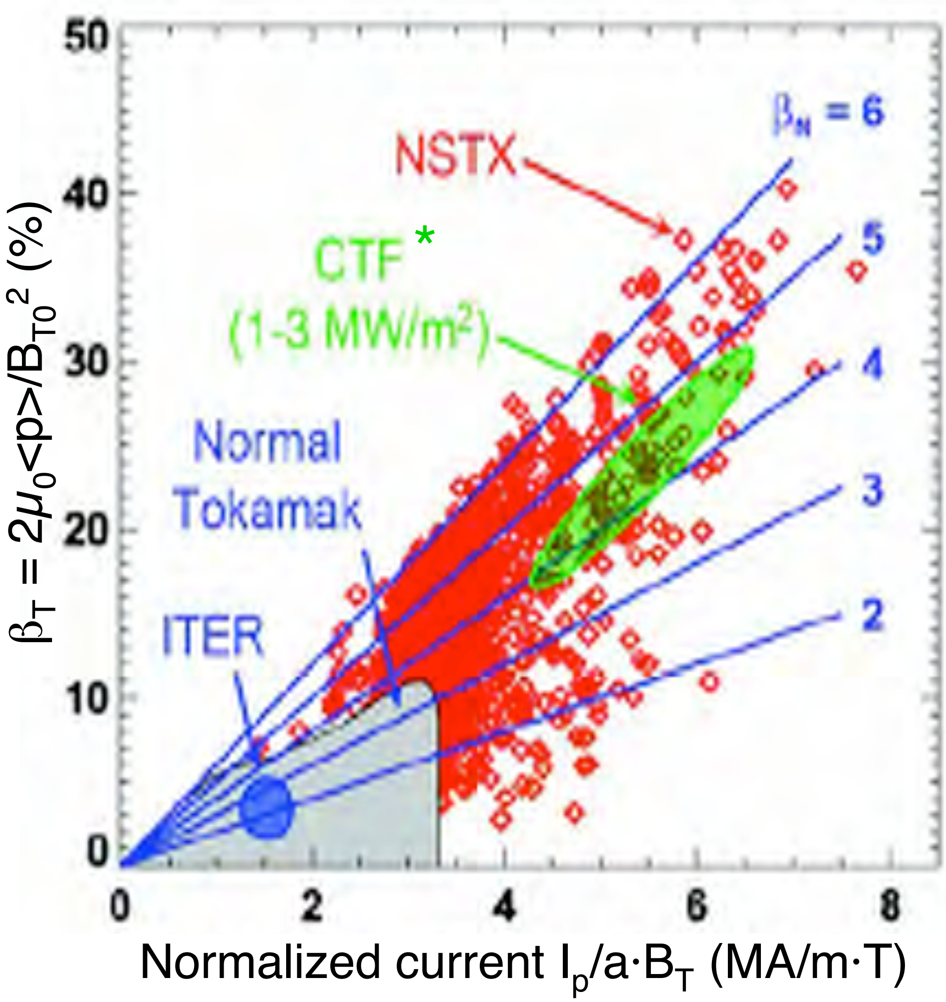

- Demonstrates benefits of
  - Low aspect ratio and cross-section shaping
  - Stabilization of MHD modes by nearby **conducting plates**
  - Active feedback suppression of MHD instabilities

* CTF: Operating regime of a possible ST-based fusion "Component Test Facility"

Data courtesy S. Sabbagh et al.

Both Boundary Shaping and Profile Variations Impact Reliability of High-β_N Operation

Boundary Shaping Effects

- Define a shape parameter* S

$$S = \frac{q_{95} I_P}{a B_T} \propto \frac{\left(1+\kappa^2\right)}{A} f\left(\kappa, \delta, \varepsilon, \ldots\right)$$

  - "How much safety factor (q_{95}) does the shape have for given I_P and B_T"
- Pulse-average β_N maximized for large values of S

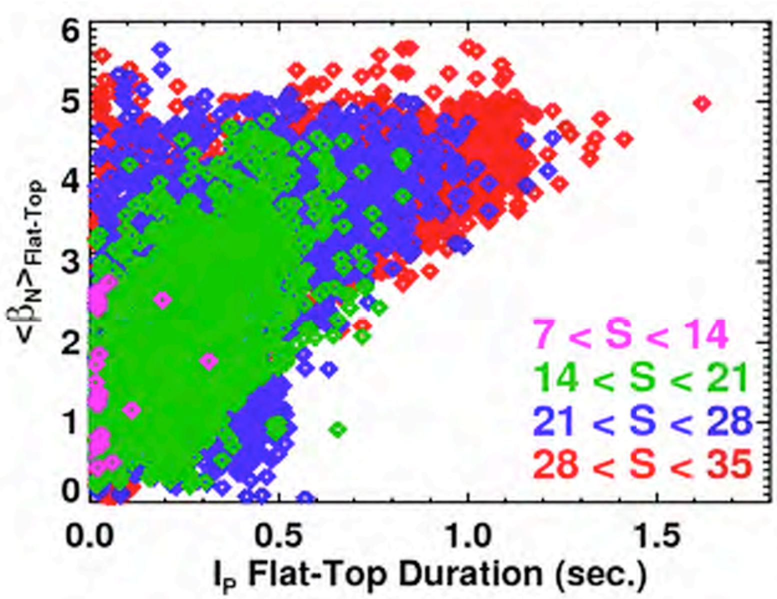

* Lazarus, et al, Phys. Fluids B 1991

Pressure Profile Shape Effects

- β_N limit calculated to scale inversely with the pressure peaking

$$F_P = \frac{P_0}{\langle P \rangle}$$

- Observations support this dependence
- H-mode produces a broad pressure profile by creating an "edge transport barrier"

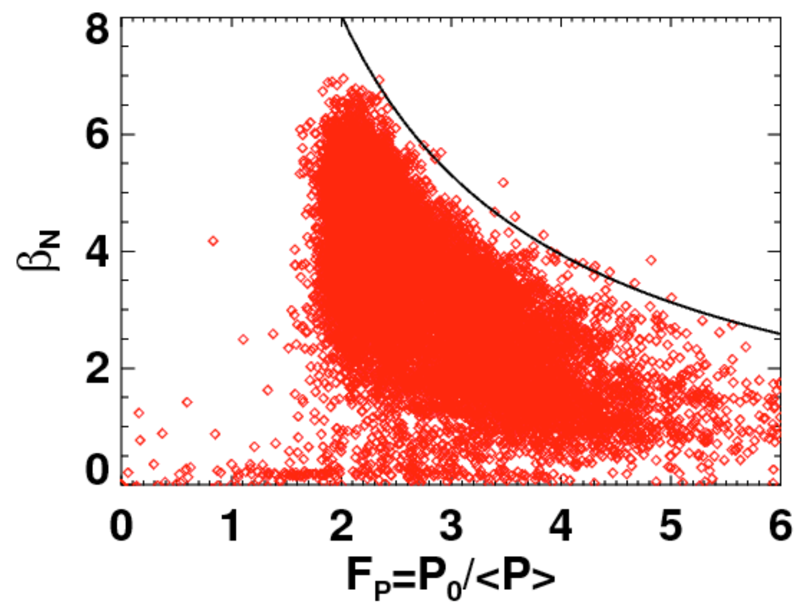

S. Gerhardt et al., *NF* **51** (2011) 073031

NSTX Achieved Non-Inductively Sustained Current Fraction up to 70% in Quiescent High-β Discharges

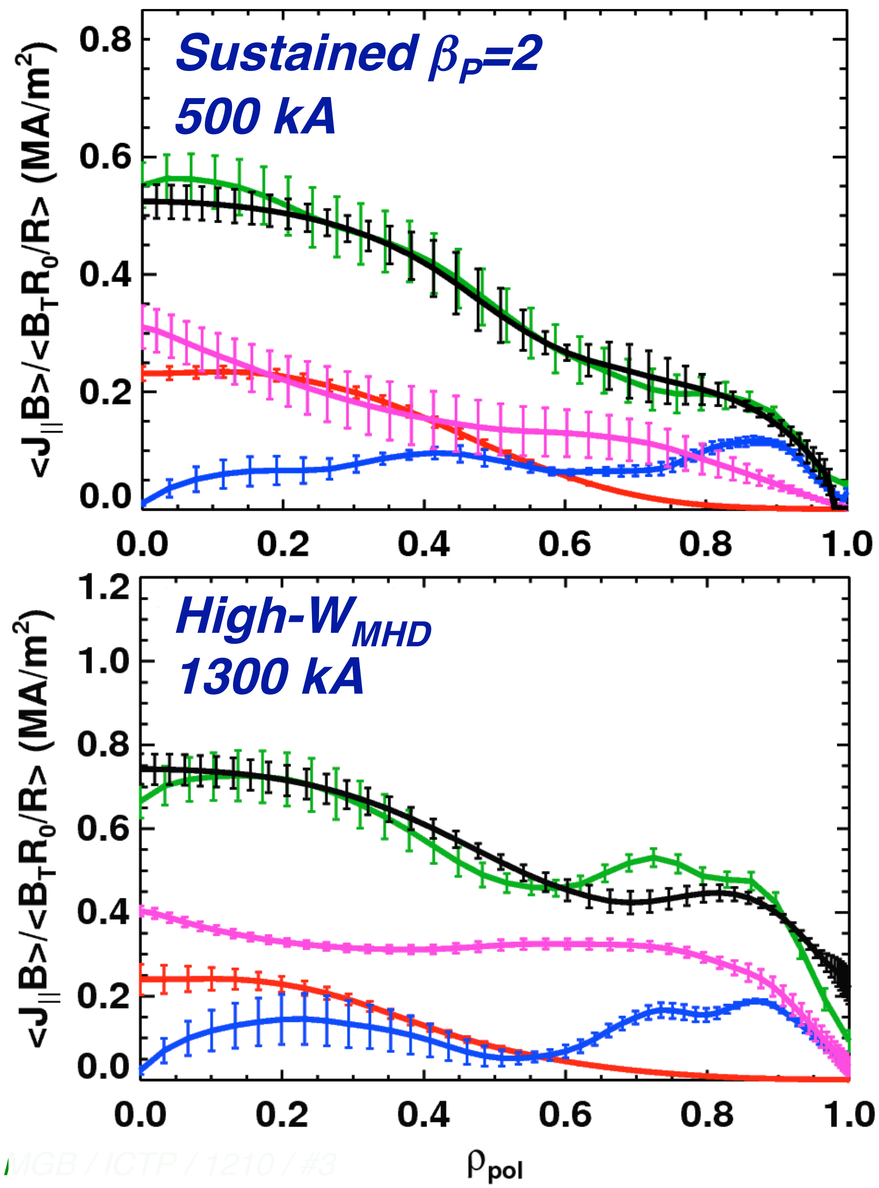

- Compare
  - **Solutions of G-S equation for J(r)** with MSE constraint

  with
  - **Modeled evolution of total current** with neoclassical resistivity, including
  - **Inductive Currents**
  - **Beam-Driven** current
  - **Pressure Driven**: Bootstrap + Diamagnetic and Pfirsch-Schlüter
- Observe good agreement when low-frequency MHD activity is absent
  - Assume classical beam ion diffusion
  - Data consistent with fast-ion radial diffusivity D_{FI} < 1.5 m²/s

S. Gerhardt et al., *NF **51** (2011) 073031*

NSTX is Equipped with Non-Axisymmetric Coils to Control MHD Instabilities at High-β

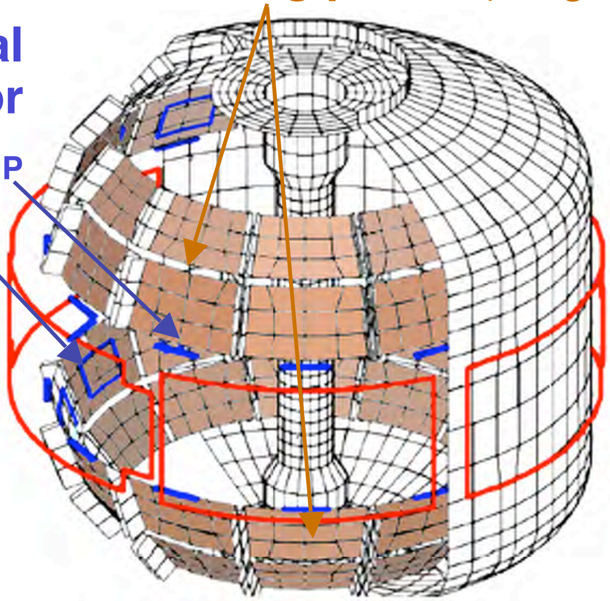

- **Conducting plates** stabilize ideal modes when β_N exceeds "no-wall" limit
- Due to finite plate conductivity, plasma can develop "Resistive Wall Mode" (RWM) on timescale for resistive decay of currents in stabilizing plates
- Plasma toroidal rotation profiles affect passive stability to RWMs
- Can suppress RWM growth by active feedback with **non-axisymmetric coils** based on real-time mode detection by **internal sensors**
  - NSTX coils generate radial field with toroidal harmonic components n = 1, 2 & 3

Correction of n = 3 Error Field Plus Feedback Control of n = 1 Mode Extends High-β_N Plasmas

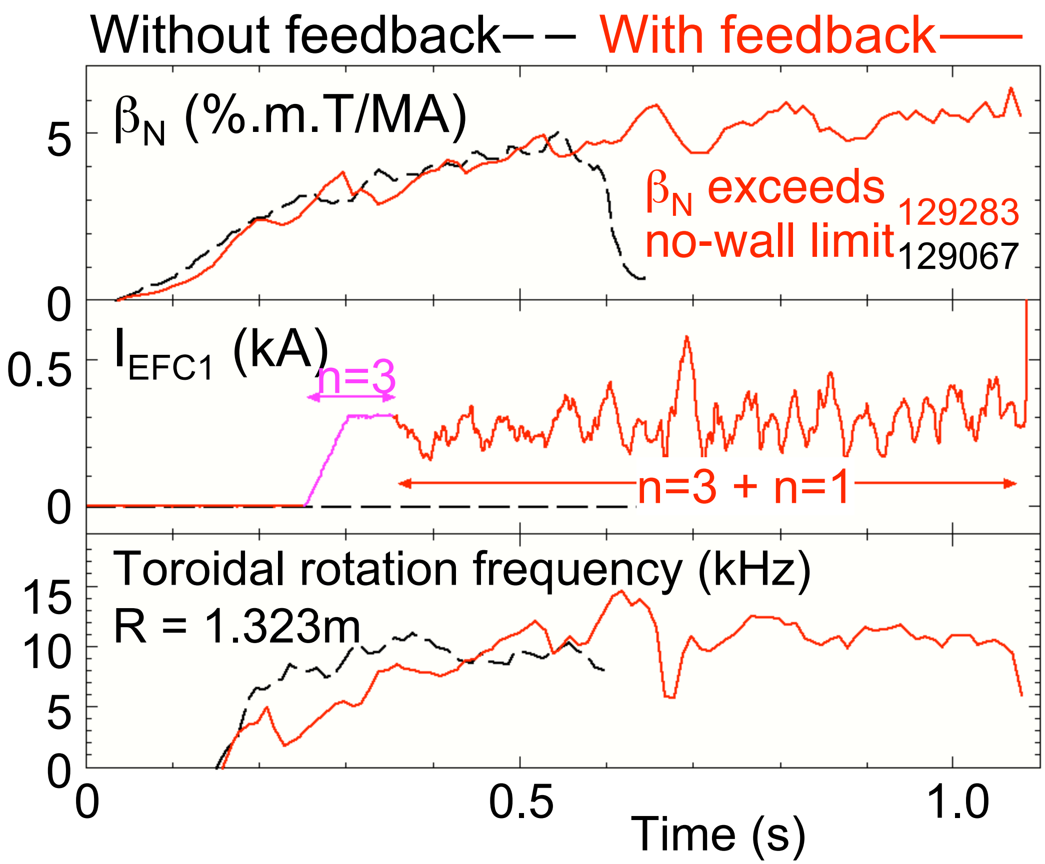

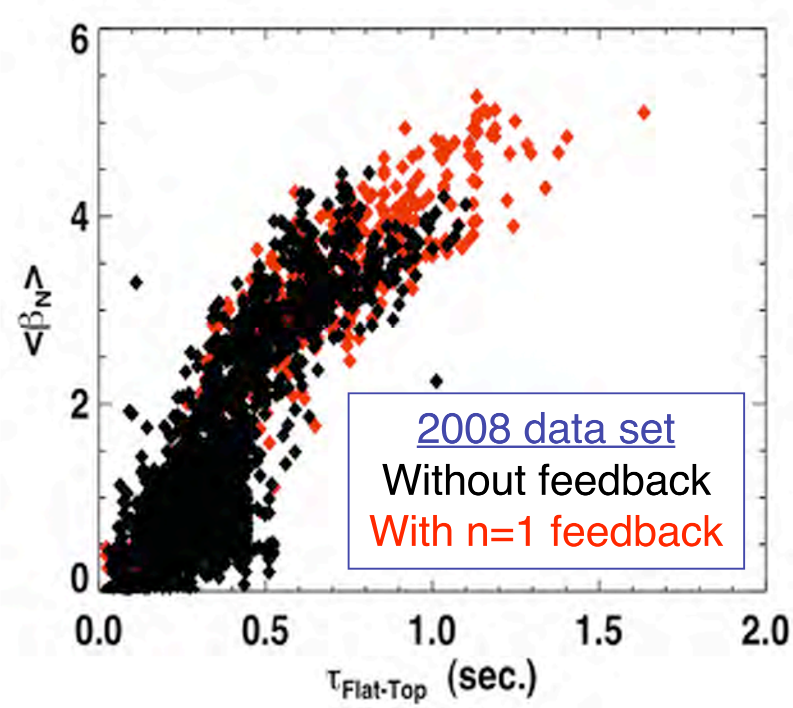

- Correction of n = 3 intrinsic error field maintains toroidal rotation
- **Resistive Wall Mode** (RWM) grows and eventually terminates discharge when normalized-β exceeds limit for plasma without conducting wall
- Application of n = 1 feedback extends high-β_N duration

S. Sabbagh et al., NF ***50*** *(2010) 025020; D. Gates et al., NF* ***49*** *(2008) 104016*

Variation of Control System Parameters Confirms Action of Feedback Loop

- Detect n=1 magnetic perturbation
  - 48 B_P, B_R magnetic sensors in vessel
  - Analyze signals in real time to obtain amplitude, toroidal phase
- Apply n=1 radial field with:
  - **Amplitude** proportional to detected perturbation
  - **Phase** shifted relative to detected perturbation
- Feedback can be changed from stabilizing to destabilizing as phase varied
- Growth of mode slows toroidal rotation by **J** × **B** force between perturbed plasma current and external fields

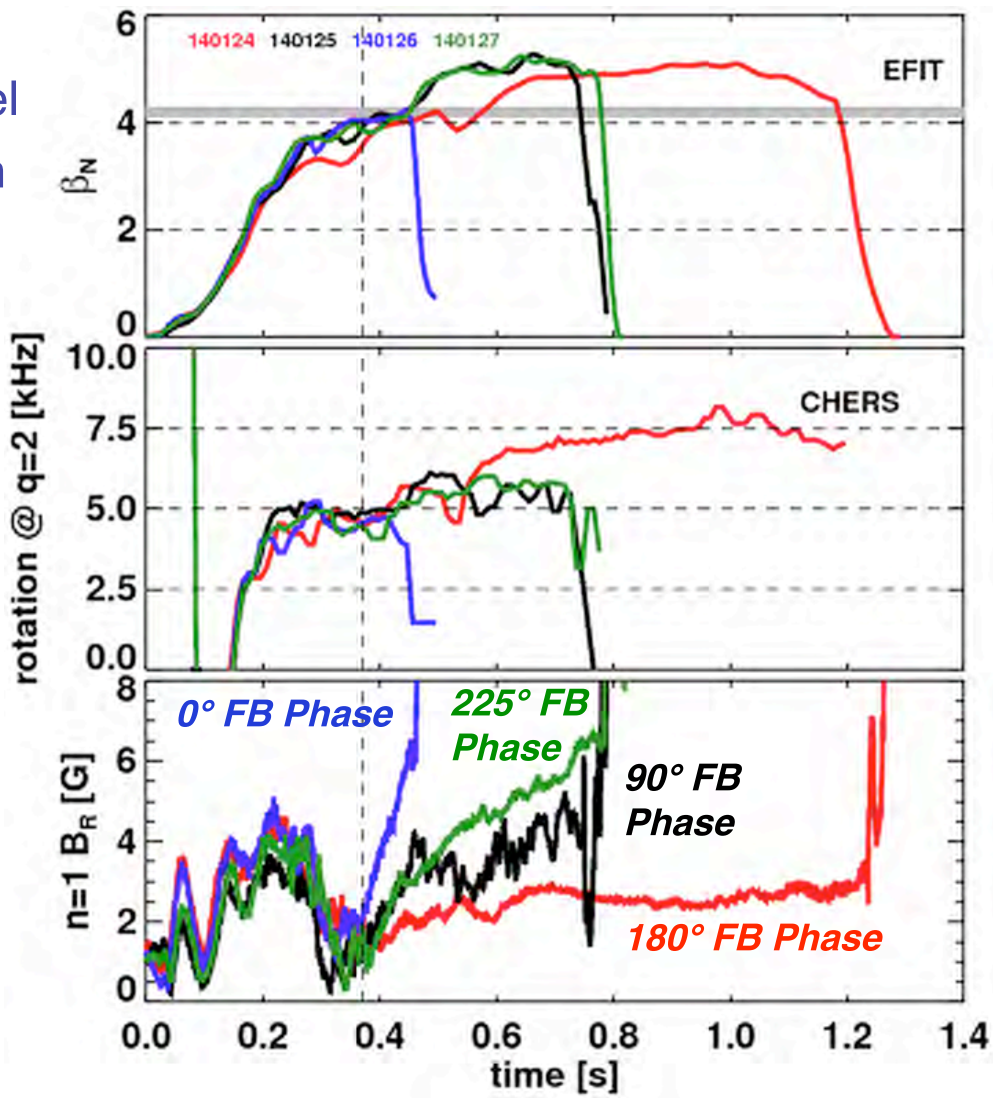

Fast Visible Images Show Plasma Asymmetry as Resistive Wall Mode Develops

Before RWM activity

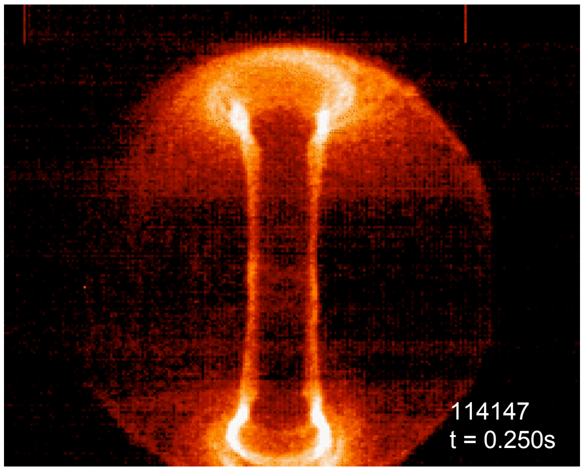

RWM with ΔB_p = 9mT

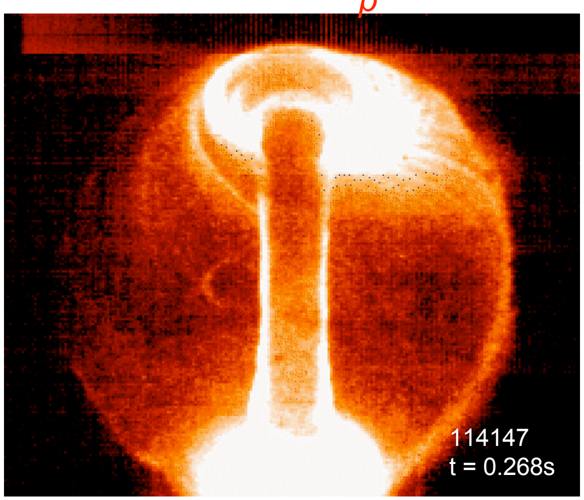

- Visible light emission comes from plasma edge
  - Core radiates in soft x-ray region
- DCON code models mode structure at boundary
  - uses experimental equilibrium
  - includes n = 1 – 3 mode components
  - uses relative amplitude / phase of n spectrum measured by RWM sensors

Modeled structure

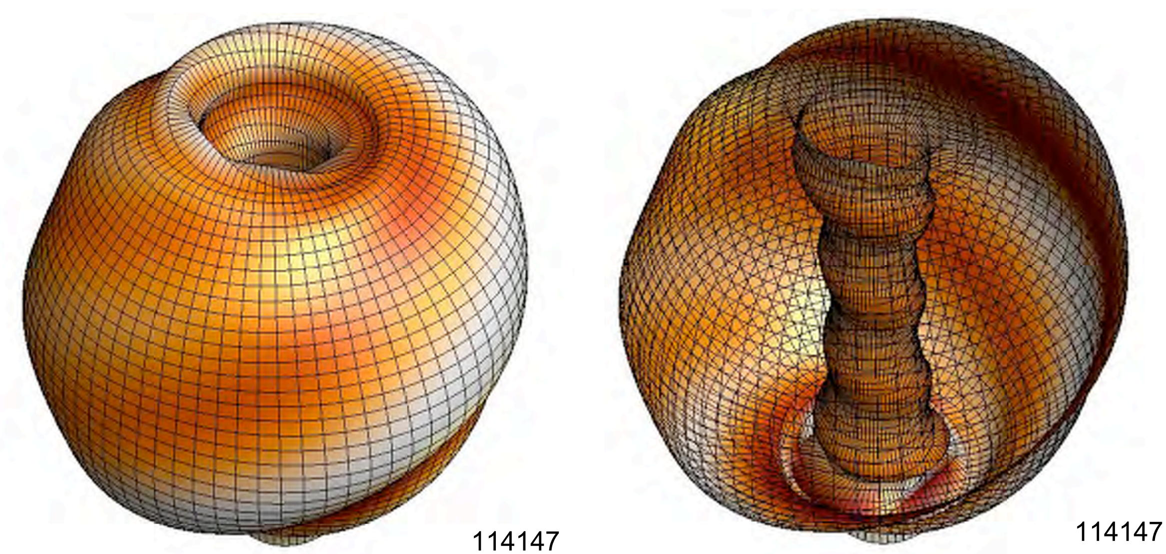

(exterior view) (interior view)

S. Sabbagh et al., *NF* ***46*** *(2006) 635*

MAST Is Equipped with Very Flexible Set of 18 Resonant Magnetic Perturbation (RMP) Coils

MAST

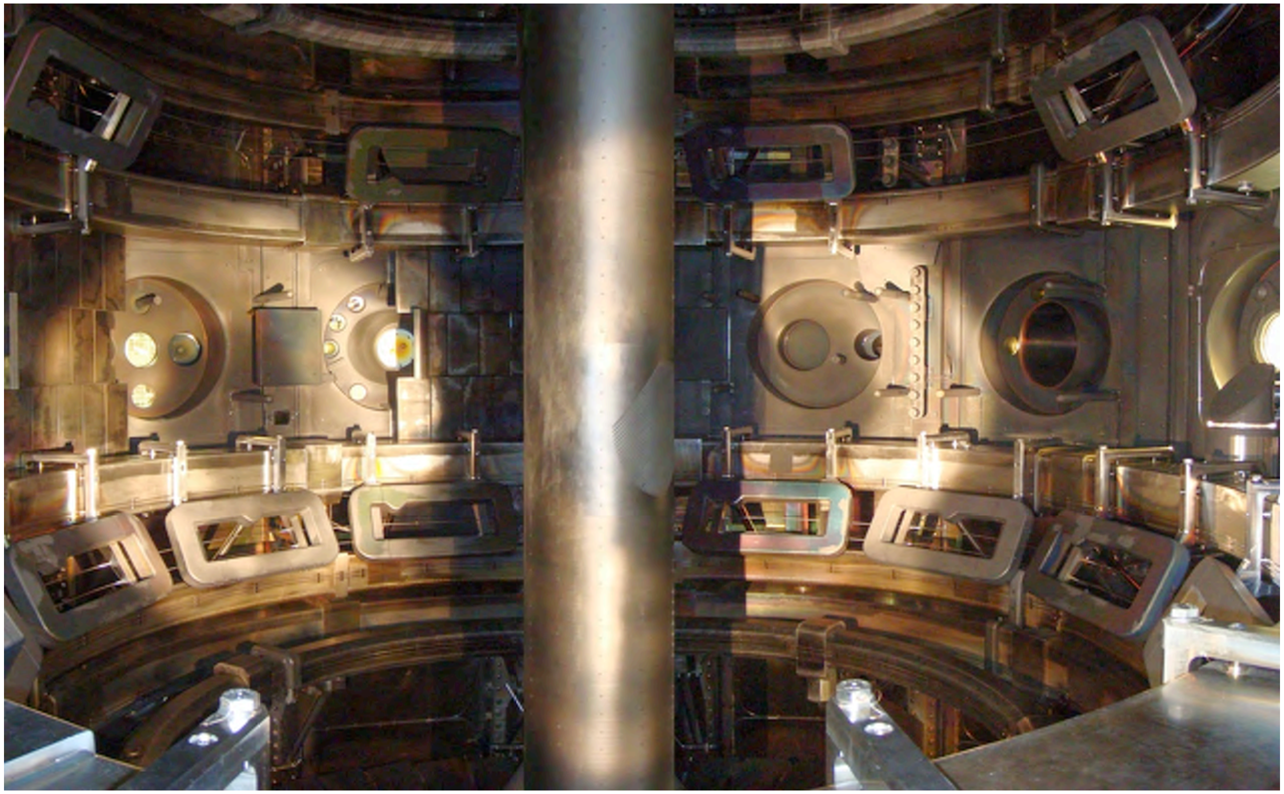

6 in upper row

12 in lower row

- Apply perturbations with toroidal harmonic up to n = 6
  - Spatial decomposition contains multiple poloidal (m) components
- Coils can be used both for control of “global” instabilities (*e.g.* kink-like modes) and modes localized to the plasma edge

MAST data courtesy of B. Lloyd and the MAST group, CCFE, UK

MAST Is Investigating Effect of RMPs on Edge Localized Modes in H-mode

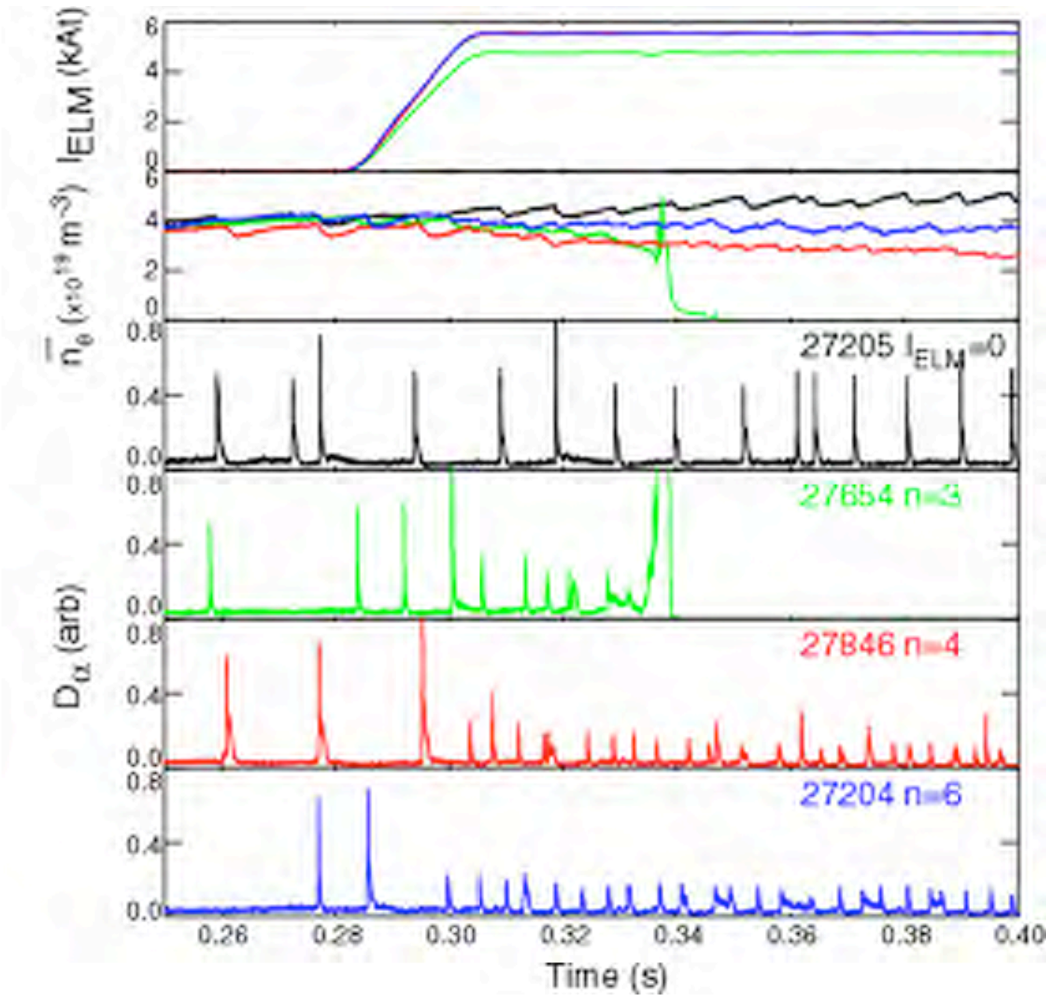

- n = 3 produces disruption
- n = 4 and n = 6 produce **ELM mitigation**
  - up to a factor of 5 increase in ELM frequency
  - similar reduction in ΔW_{ELM}
  - Edge pressure gradient is reduced by RMP
- Observe stronger braking of rotation as n = 6 → 4 → 3
- RMPs have not completely suppressed ELMs in MAST
  - Suppression achieved in conventional tokamaks *under some conditions*

Courtesy of I. Chapman and MAST group, CCFE, UK

With RMP, Obtain Good Agreement in Edge Structures Between Images and Field Line Mapping

MAST

n=6 n=4 n=3

Camera images
tangential view

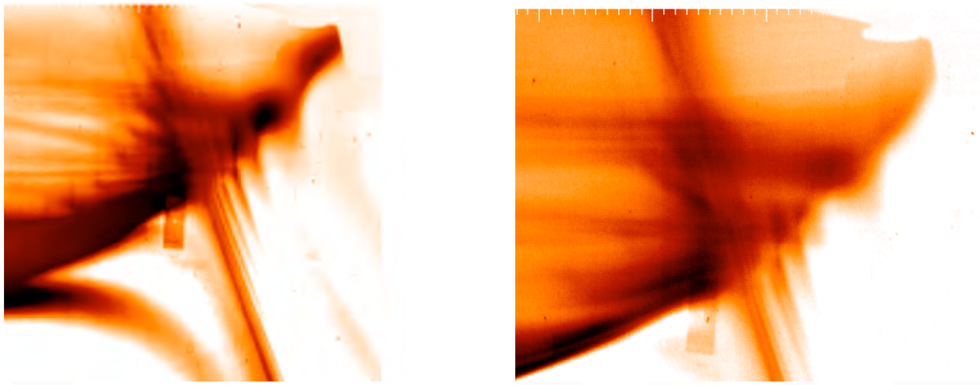

Field line mapping
ERGOS code

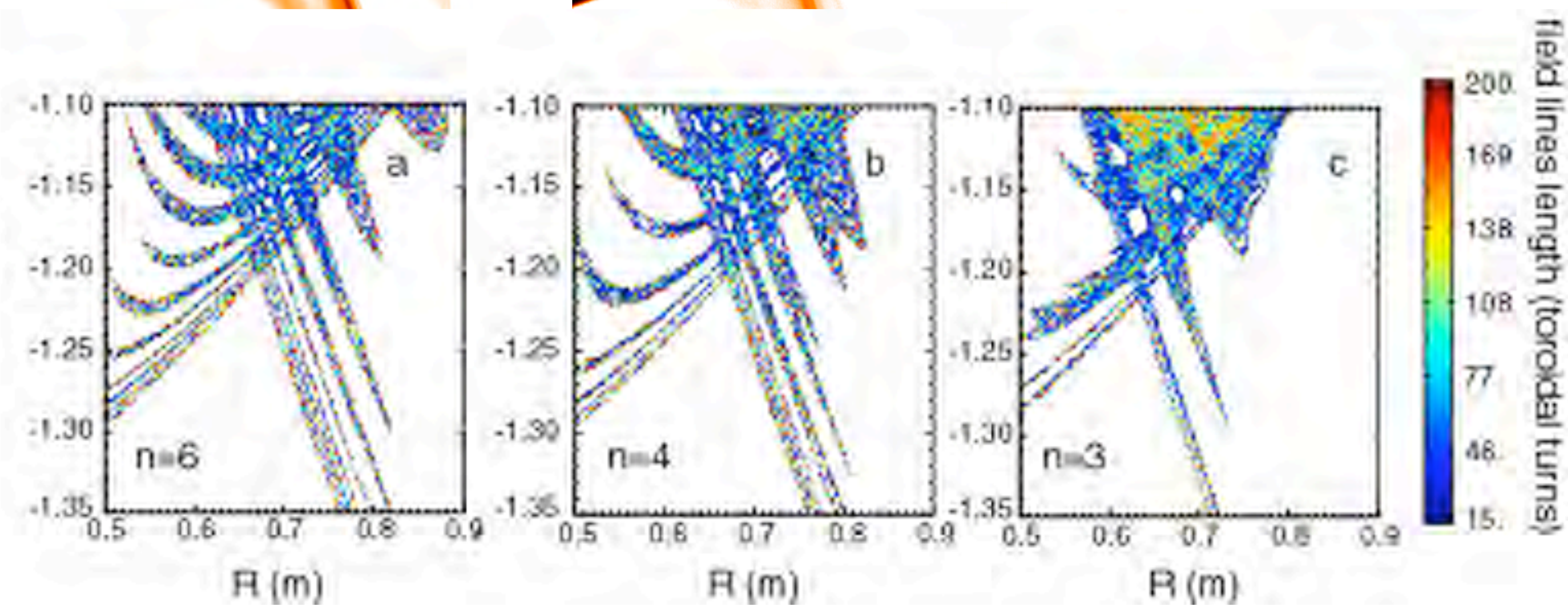

Courtesy of I. Chapman and MAST group, CCFE, UK

Application of RMP Splits the Outer Strike Point on the Outer Divertor Plate

MAST

- High spatial resolution (1mm) IR measurements of divertor plate temperature reveal the splitting as RMP is applied

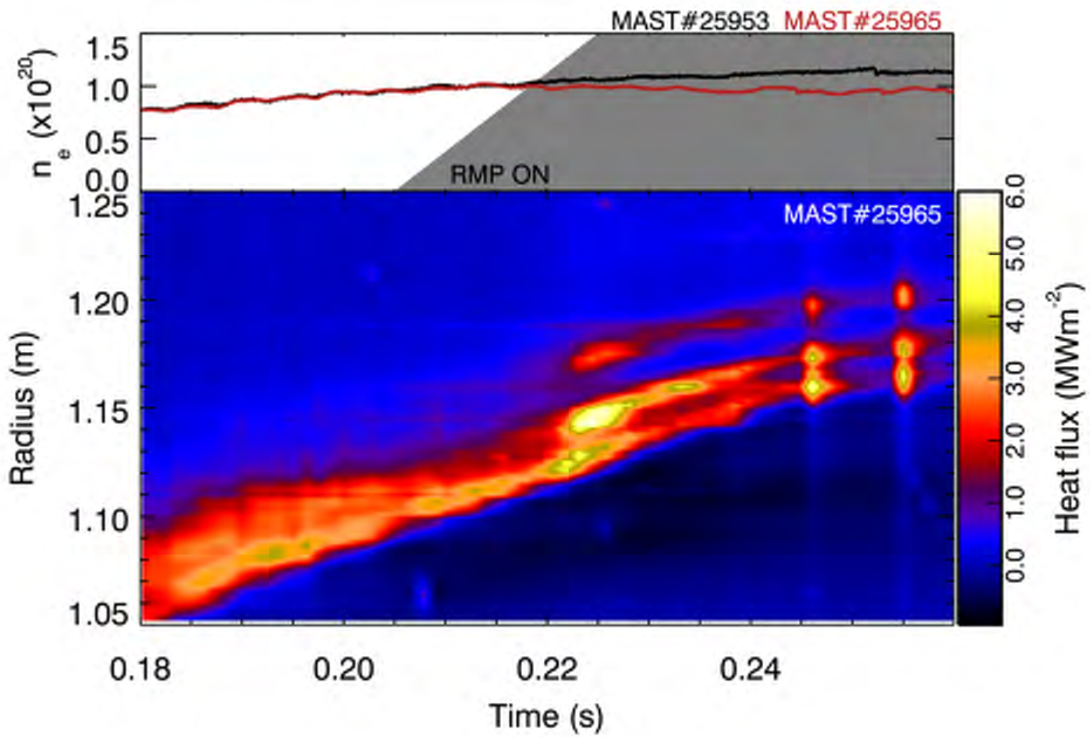

- Observed only for RMP magnitude above a threshold
  - Currents induced in plasma can shield small applied fields
- Strike point splitting coincides with onset of density reduction

Courtesy of A. Thornton and MAST group, CCFE, UK

Reducing Heat Flux on the Divertor Critical for the Success of the ST

- Power flux scaling parameter: $P_{SOL}/(R_{SP}\delta_{SOL})$

  P_{SOL}: scrape-off layer power

  R_{SP}: major radius of divertor "strike-point" (separatrix intersects divertor)

  δ_{SOL}: cross-field width of the scrape-off layer in divertor

  – Intrinsically high in the ST due to high power and small size
  – δ_{SOL} scales roughly as $\sim I_p^{-1}$ in both STs and conventional tokamaks
- Can address problem through all three factors
  – Reduce P_{SOL} by radiation both from core plasma and locally in divertor
  – Maximize δ_{SOL} by changing magnetic geometry of the divertor
  – Increase R_{SP} by leading outer leg of the separatrix to larger major radius
- Ultimately a combination of techniques plus the development of resilient divertor materials will probably be needed
  – Divertor surface may need to be "self healing" (*e.g.* liquid metals) to survive off-normal transient events

Plasma Shaping Reduces Peak Divertor Heat Flux in NSTX

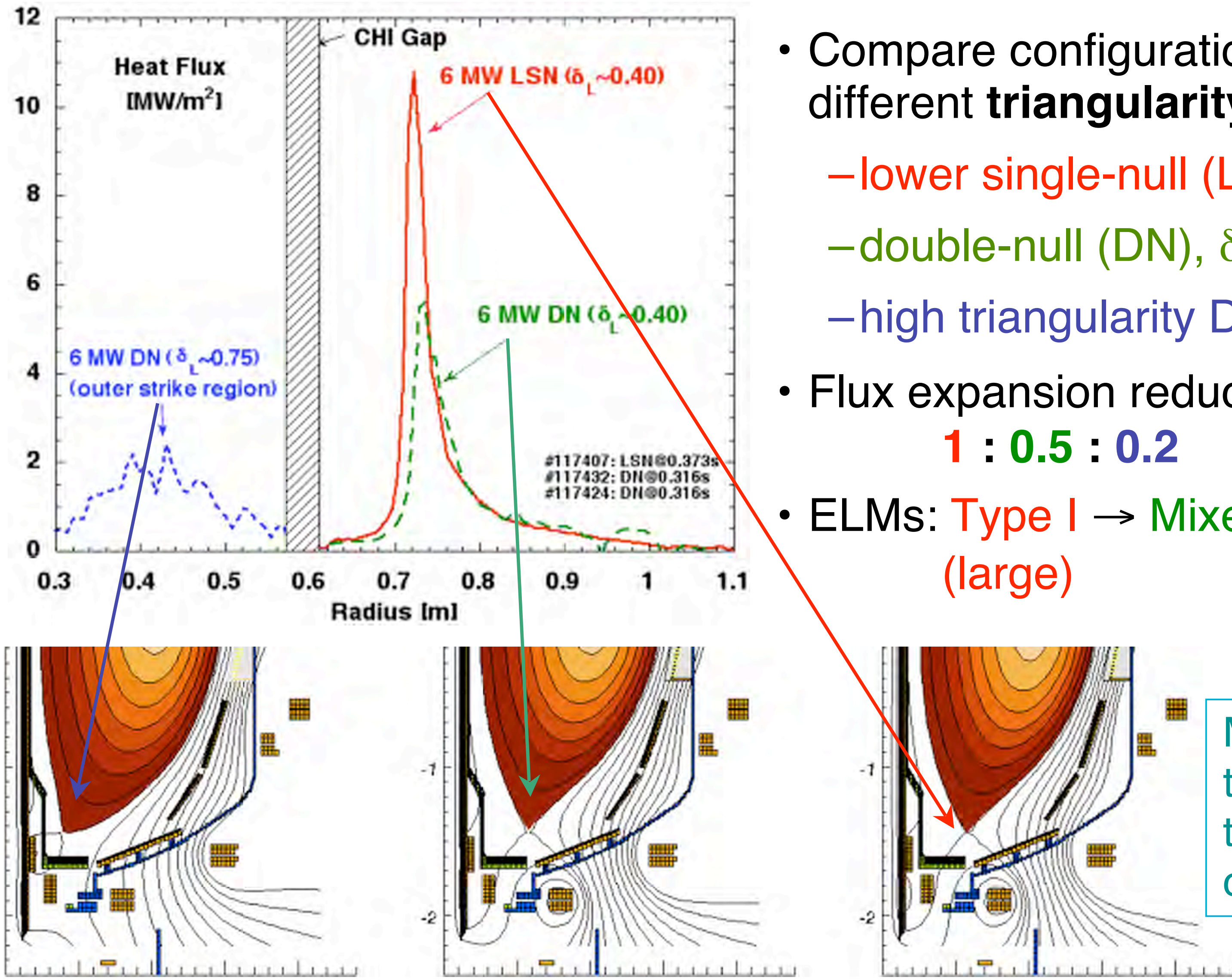

- Compare configurations with different **triangularity** at X-point δ_X
  - lower single-null (LSN), $\delta_X \approx 0.4$
  - double-null (DN), $\delta_X \approx 0.4$
  - high triangularity DN $\delta_X \approx 0.75$
- Flux expansion reduces heat flux
  1 : 0.5 : 0.2
- ELMs: Type I → Mixed → Type V
  (large) (small)

Measure heat flux to divertor with IR thermography of carbon tiles

*R. Maingi, J. Nucl. Mat. **313-316** (2003) 1005*

Partial Divertor Detachment by Divertor Gas Puffing Reduces Peak Heat Flux Without Degrading Core

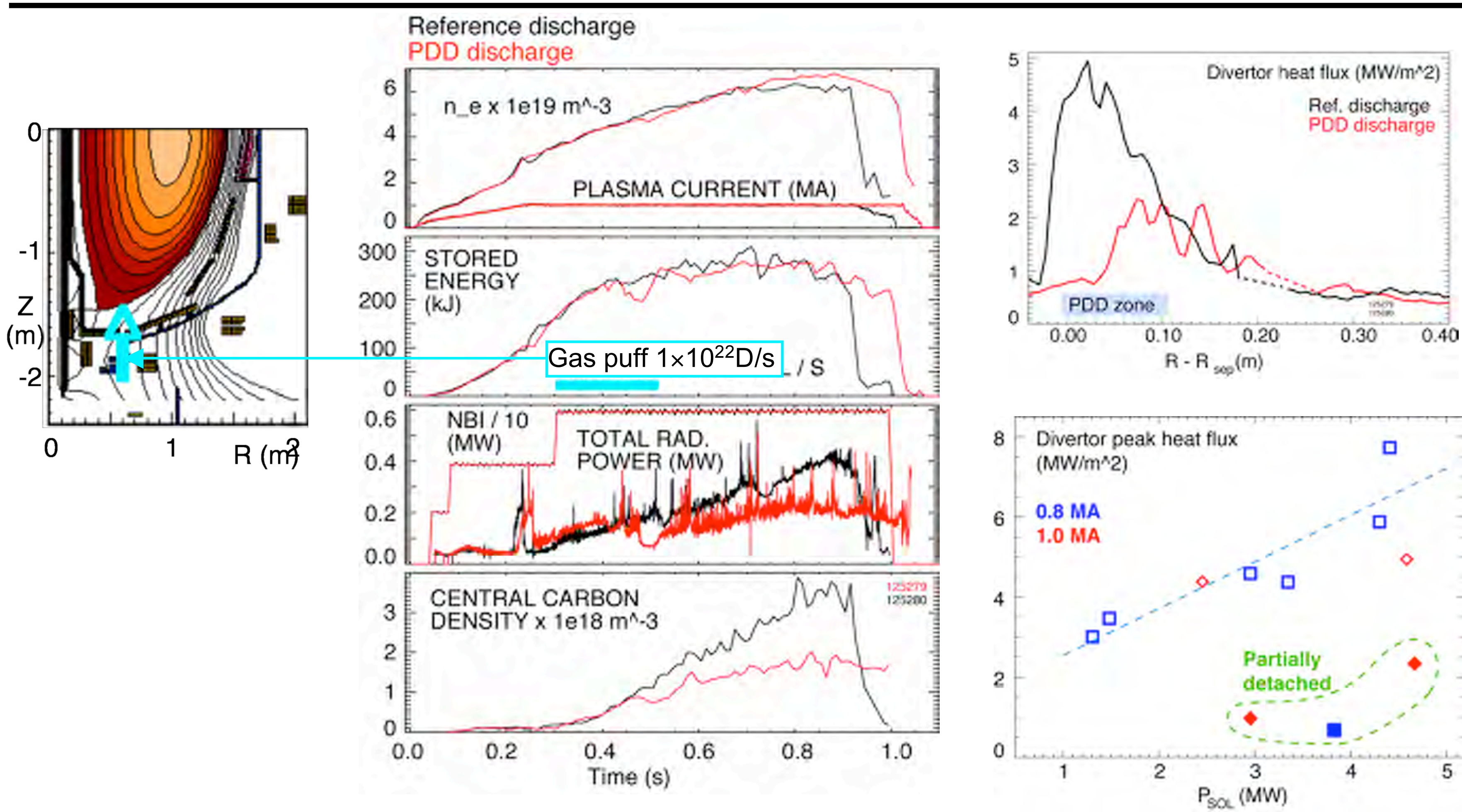

- Intense gas puff creates region of **dense radiating plasma** near divertor
- Core radiation and carbon density are **reduced** during partial detachment

"Snowflake" Divertor Produced Significant Heat Flux Mitigation in NSTX

- Energize additional PF coils in the divertor to create a *hexapole* field null
  - Single divertor coil produces a *quadrupole* field null
- Snowflake divertor experiments with P_{NBI}=4 MW, P_{SOL}=3 MW
  - Kept good H-mode confinement
  - Peak divertor heat flux reduced from **3 – 7** to **0.5 – 1** MW/m^2
  - Due to combination of snowflake divertor configuration and outer strike-point "detachment" as divertor radiation rises

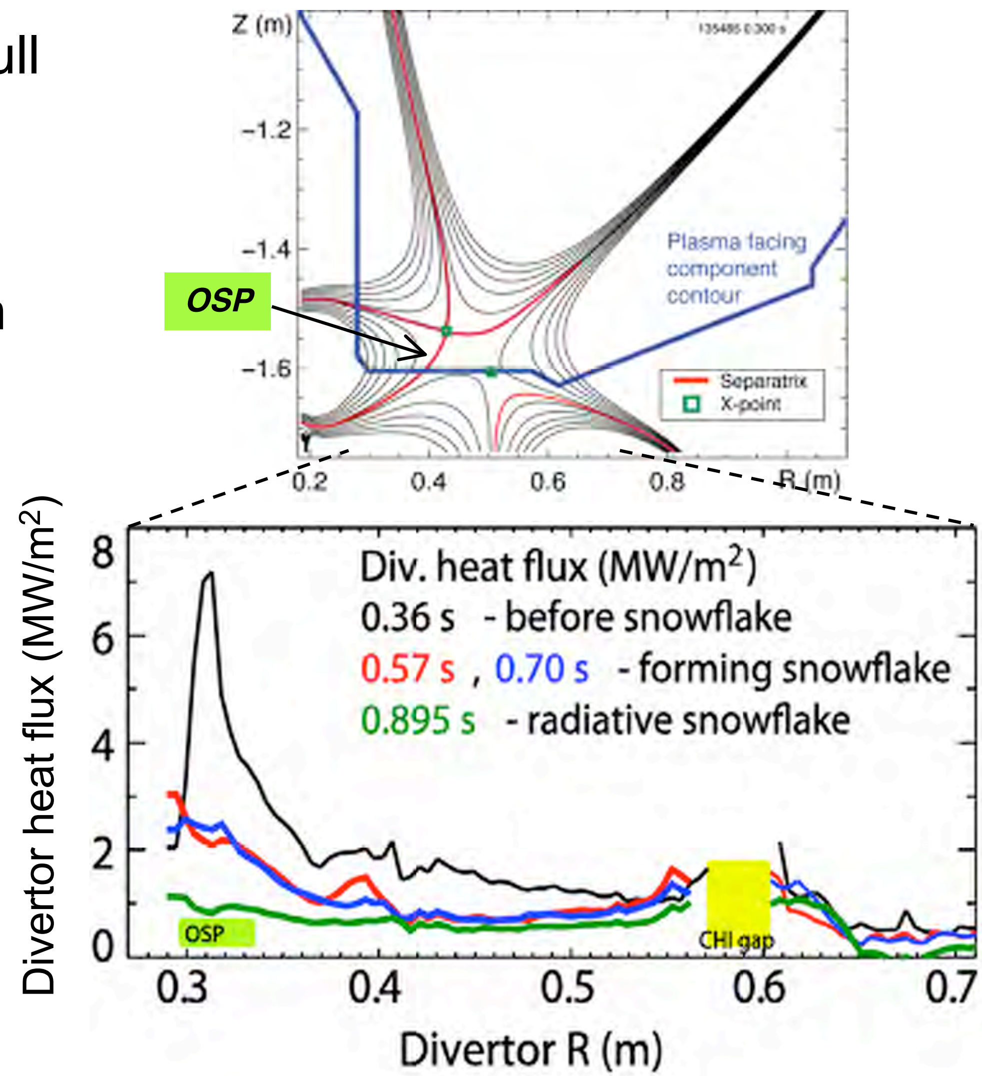

V. Soukhanovskii et al., PoP **19** (2012) 082504

MAST Will Install Additional Internal PF Coils to Produce an Extended or "Super-X" Divertor

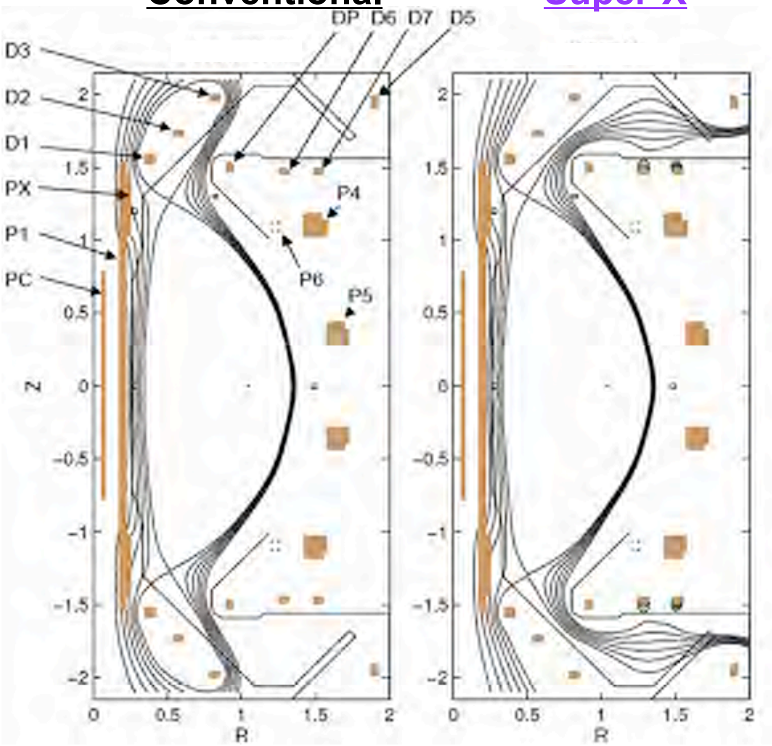

Simulation of plasma in Super-X divertor

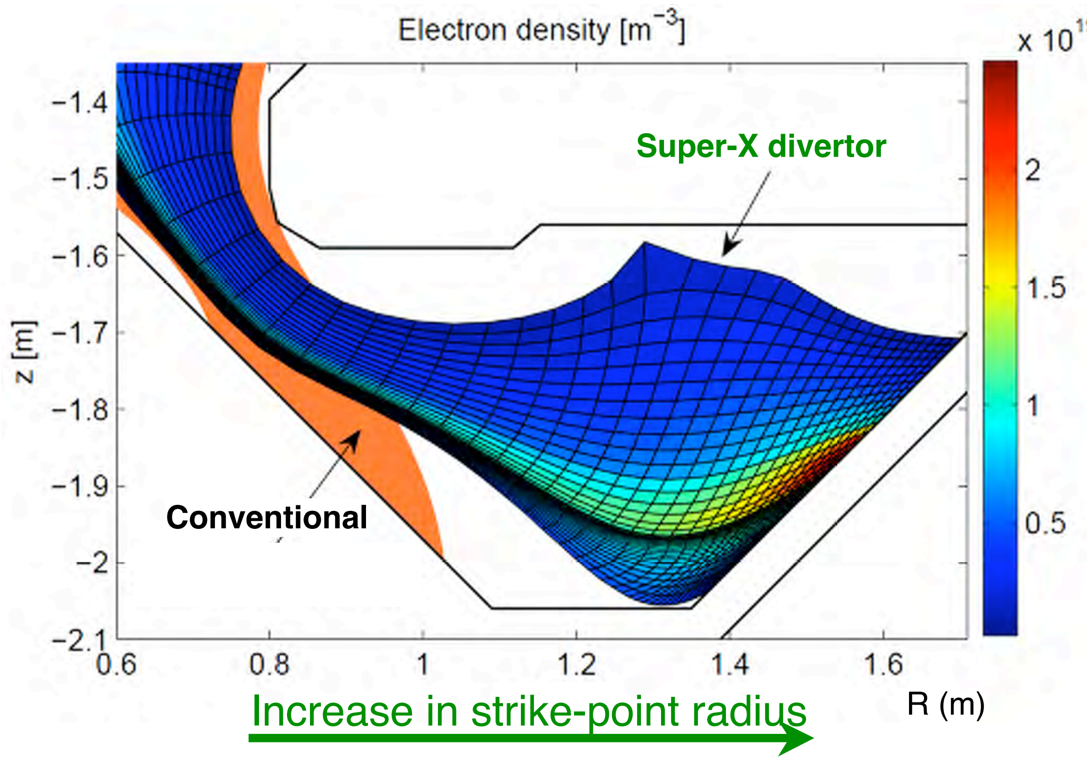

- Physics to be studied:
  - reducing divertor heat loads by radiation and spreading strike zone
  - impact on H-mode access, structure of pedestal and ELMs
  - turbulence and transport in SOL
  - impurity migration and effects on radiation in core and divertor
  - propagation and effects of non-axisymmetric phenomena from core

 Courtesy of J. Milnes, W. Morris and MAST group, CCFE, UK *P. Valanju, PoP **16** (2009) 056110*

NSTX Has Explored Use of Lithium Coating on Plasma Facing Components (PFCs)

- Started with lithium pellet injection: applied 5 - 25mg
- Developed dual lithium evaporators (LITERs) to coat lower divertor
- Evaporate 1 – 80 mg/min with lithium reservoirs at 520 – 630°C for 7 – 15 min between discharges
- Shutters interrupt lithium deposition during discharges
- Withdrawn behind airlocks for reloading with lithium

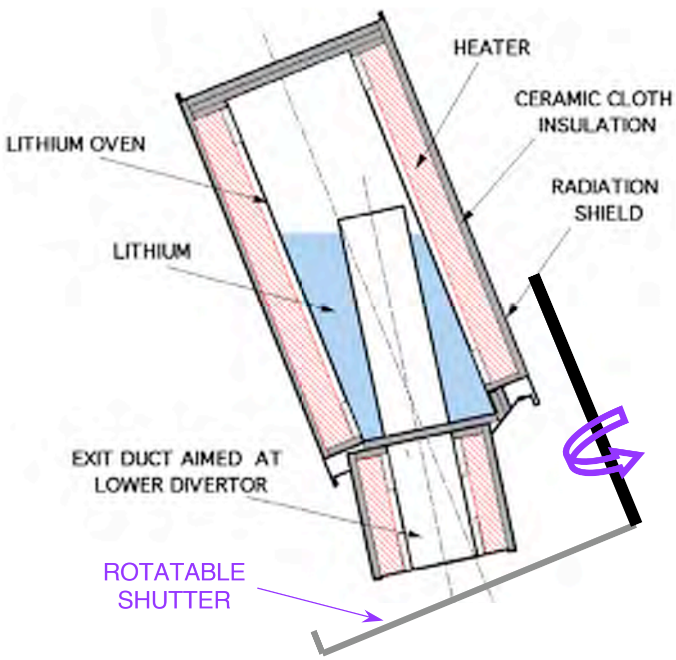

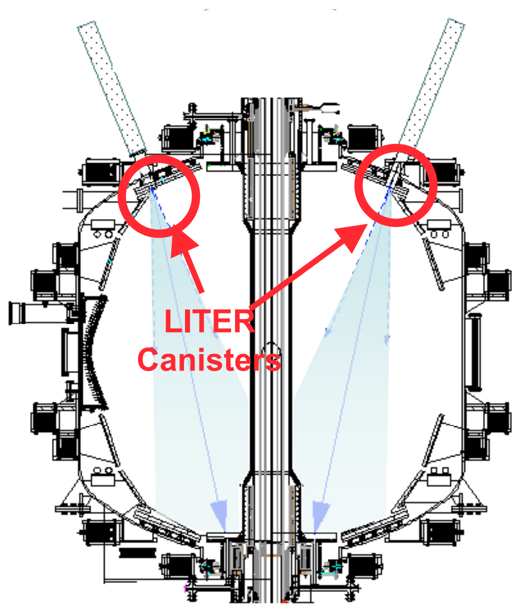

Modeled deposition pattern

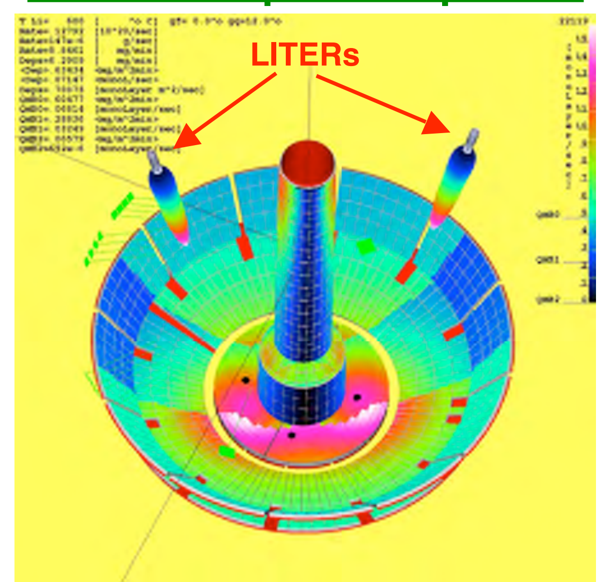

Lithium Coating Reduces Deuterium Recycling, Suppresses ELMs, Improves Confinement

No lithium (129239); **260mg lithium** (129245)

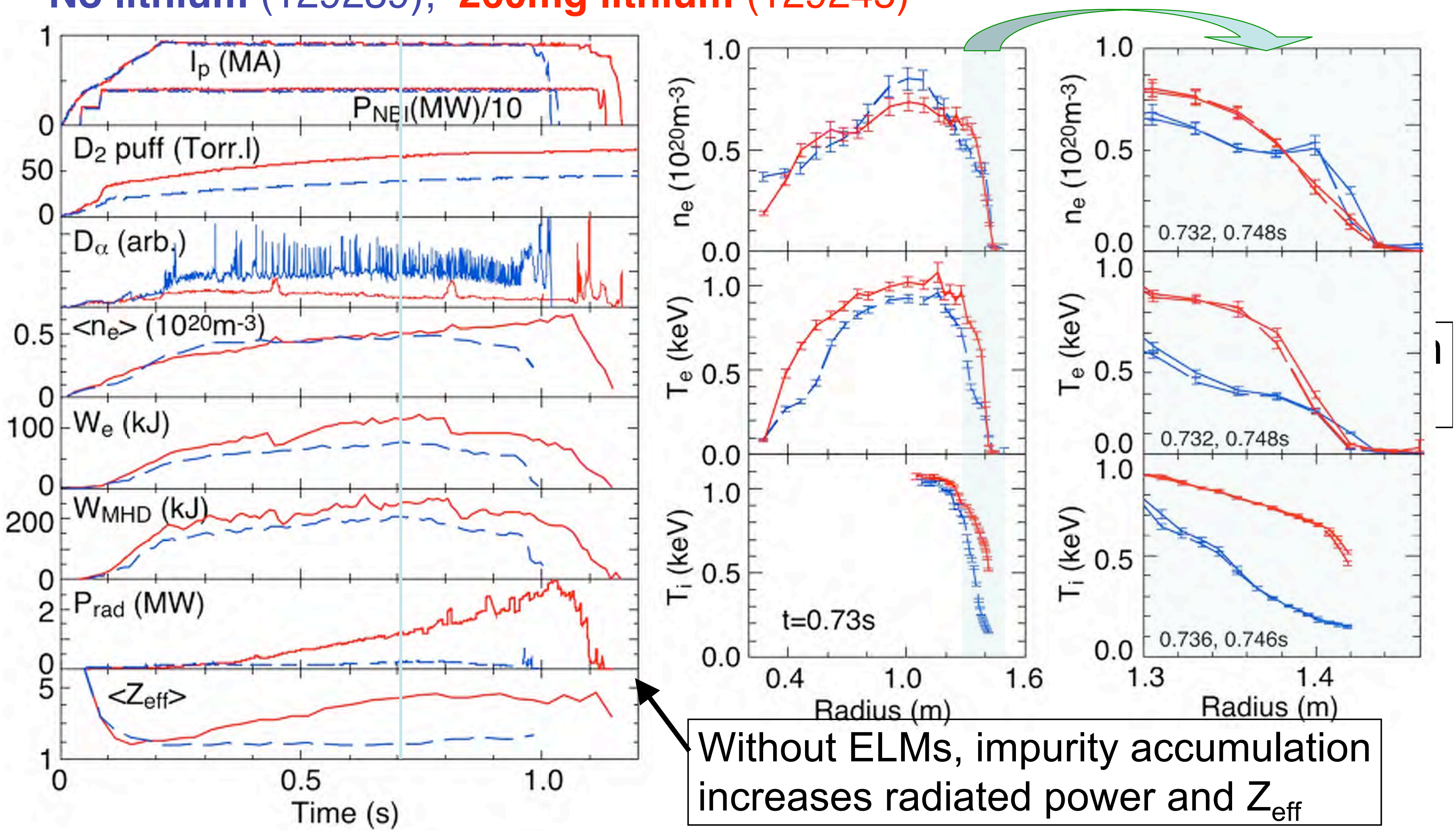

Without ELMs, impurity accumulation increases radiated power and Z_{eff}

M.G. Bell et al., PPCF 51 (2009) 124054

Lithium Coating Improves Both Total and Electron Confinement

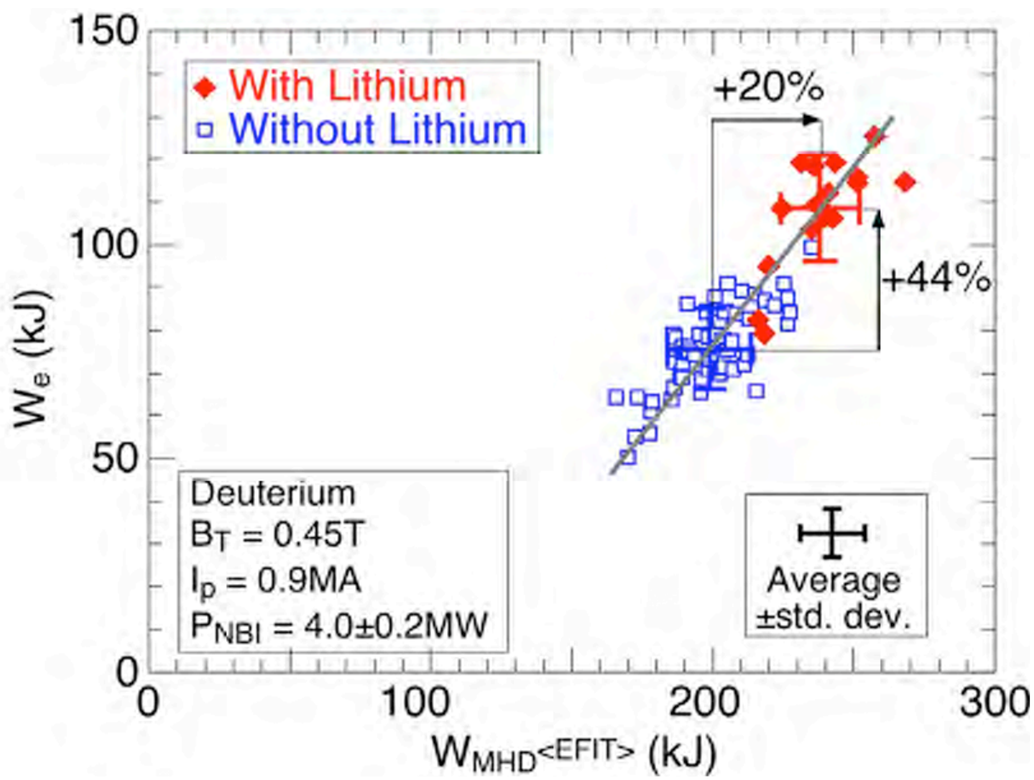

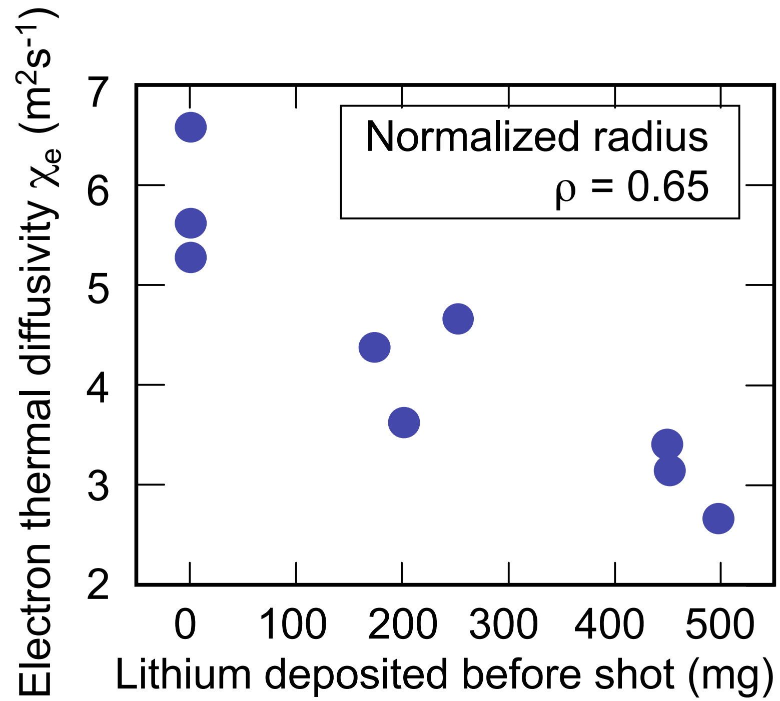

- H-mode threshold reduced by lithium by up factor 4
- Electron temperature profile becomes broader with lithium
- Electron thermal transport in outer region progressively reduced by lithium
- Ion confinement remains close to neoclassical both with and without lithium

S. Ding et al., PPCF ***52*** *(2010) 015001*

Lithium Affects ELMs Through Changes in Temperature and Pressure Profile at Edge

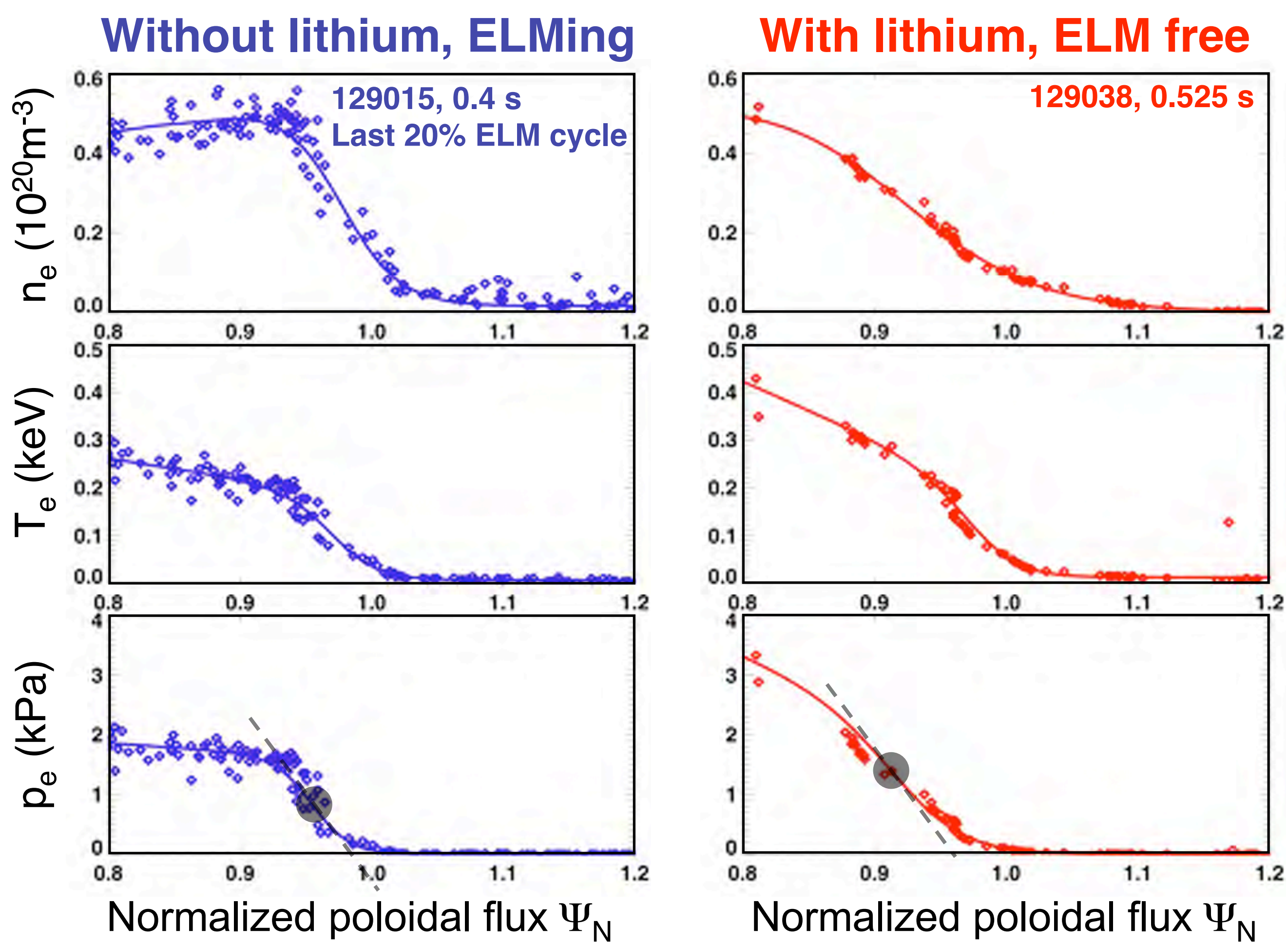

- Shift of maximum in pressure gradient to region with lower magnetic shear ($\partial q/\partial r$) stabilizes kink/ballooning instability at edge

R. Maingi et al. *PRL* ***103*** *(2009) 075001*

External Non-Axisymmetric Coils Can *Induce* Repetitive ELMs in Discharges with Lithium Coating

κ=2.4, δ=0.8, 0.8MA, 0.45T, NBI 4 MW

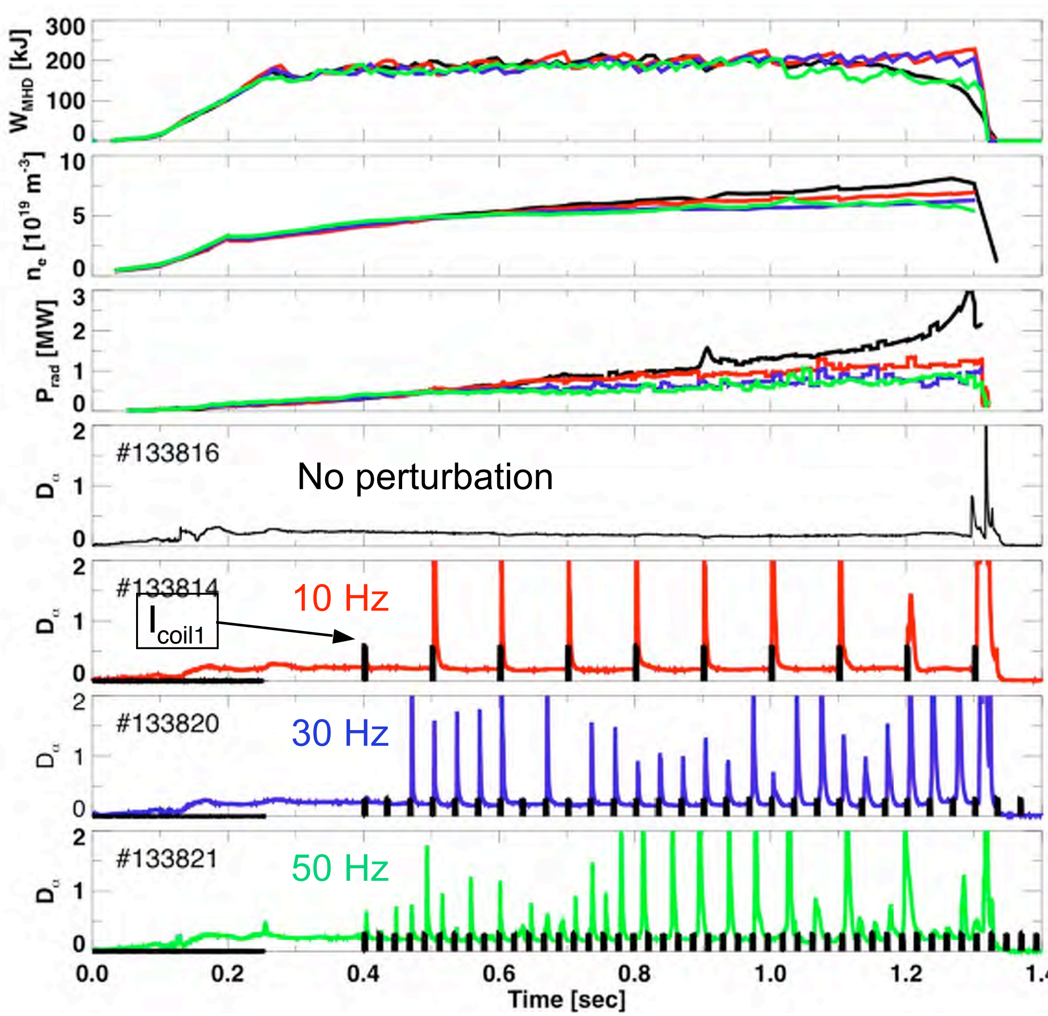

- Applied n = 3 resonant radial field perturbations with NSTX RMP coils
- Induced ELMs reduce n_e, P_{rad}, Z_{eff} with small effect on plasma energy

J. Canik et al., *NF* ***50*** *(2010) 064016*

STs Provide New Opportunities to Study Physics of Toroidal Transport Processes

- Operate in unique regions of dimensionless parameters
  - Normalized gyro-radius ρ^*, normalized collisionality ν^*
  - Range of β spans electrostatic to electromagnetic turbulence
- Analysis of NSTX data demonstrated that ion transport was close to neoclassical and that electron transport determined core confinement
  - Suppression of ion turbulent transport at low B had been postulated

Ion thermal diffusivity

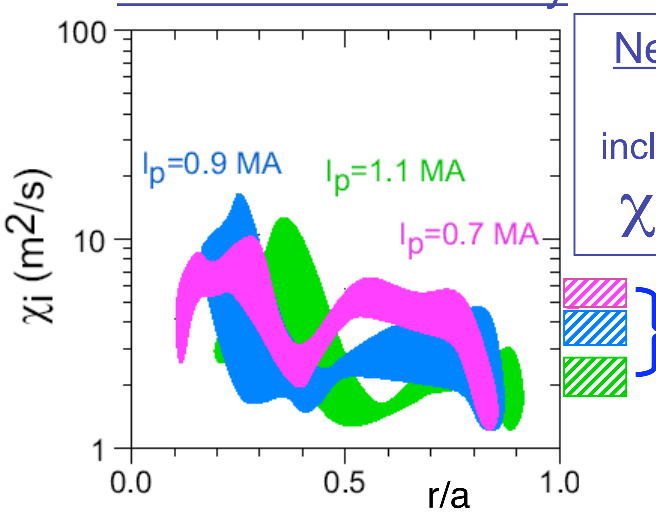

Neoclassical calculation
(GTC-NEO code)
including finite banana width
χ_i (r/a=0.5-0.8) $\propto I_p^{-1}$

Electron thermal diffusivity

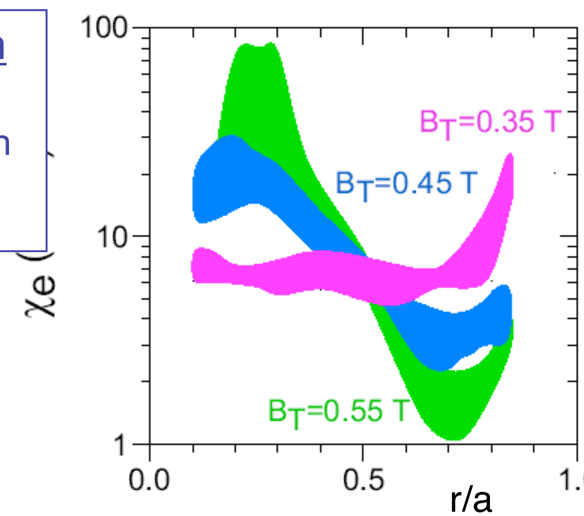

- Dependence of electron transport on B-field was a surprise
- Low B $\Rightarrow$ electron gyro-scale turbulence should be measurable ($\rho_e \sim 0.1$ mm)

S. Kaye et al., *NF* ***46*** *(2006) 848*

With Lithium Coated PFCs, Global Confinement Trends are Similar to Conventional Aspect Ratio

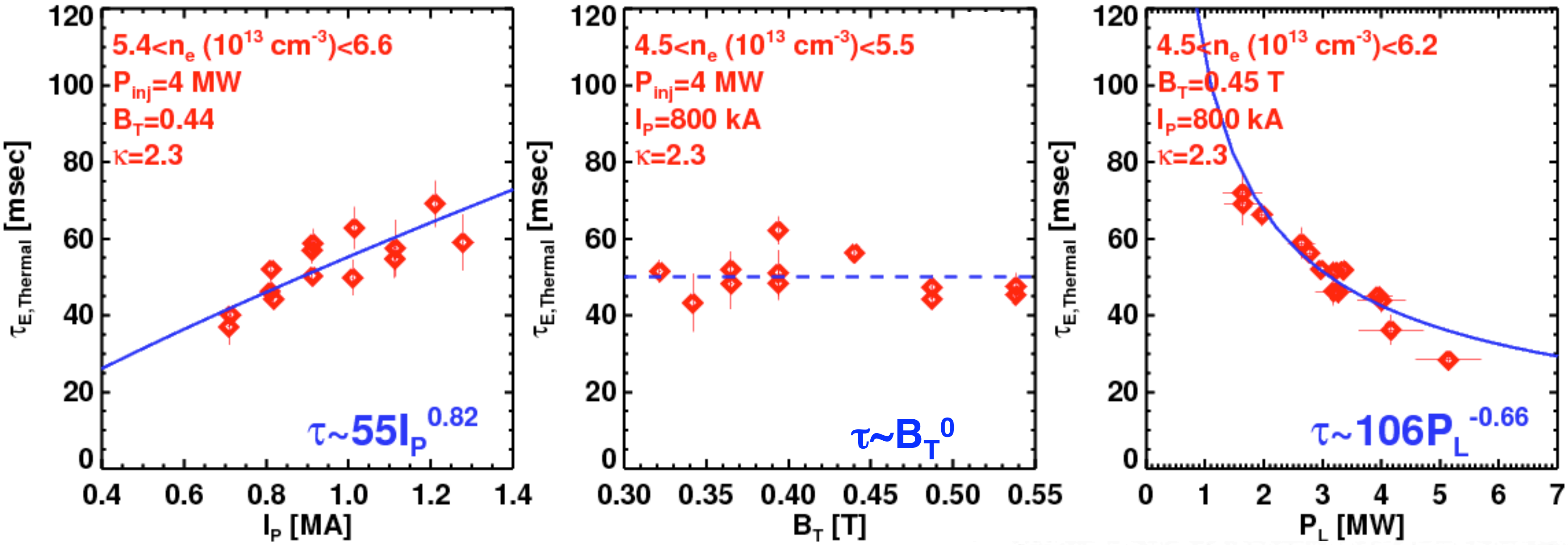

- Compare experimental confinement time with prediction from ITER 1998 scaling

$$\tau_{E,98} \propto I_P^{0.93} B_T^{0.15} \bar{n}_e^{0.41} P_{Loss}^{-0.69} R_0^{1.97} \varepsilon^{0.58} \kappa^{0.78}$$

- Prior to use of lithium, NSTX confinement showed weaker I_P, stronger B_T dependence

$$\tau_{E,ST} \propto I_P^{0.57} B_T^{1.08} \bar{n}_e^{0.44} P_{Loss}^{-0.73}$$

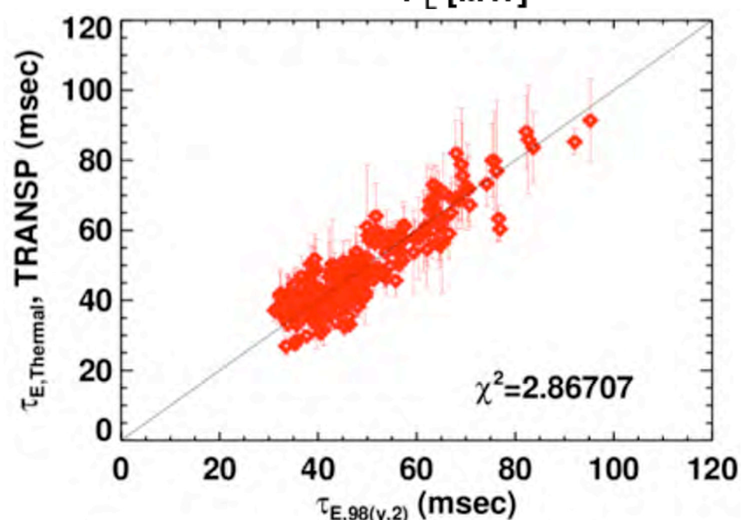

S. Gerhardt et al., *NF* ***51*** *(2011) 073031*

NSTX Equipped with Diagnostics to Measure Turbulent Density Fluctuations

- Density fluctuations ⇒ potential fluctuations ⇒ $\tilde{\mathbf{v}} = \tilde{\mathbf{E}} \times \mathbf{B}/B^2$ ⇒ **transport**
- Probe density fluctuation structures perpendicular to B-field; $\mathbf{k}_\perp \neq \mathbf{0}$
  - Structures are extended along B-field: $\mathbf{k}_{||} \approx \mathbf{0}$

Beam Emission Spectroscopy

Detect fluctuations in Doppler-shifted D_α line from excited beam neutrals

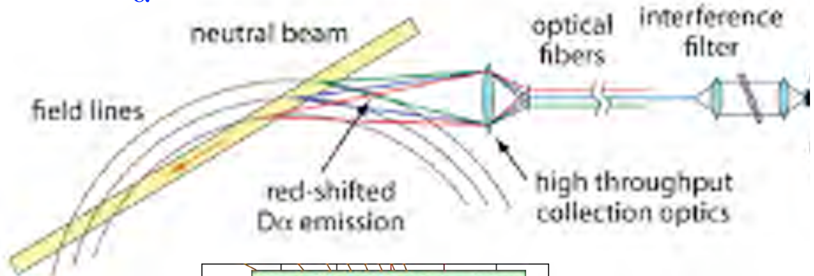

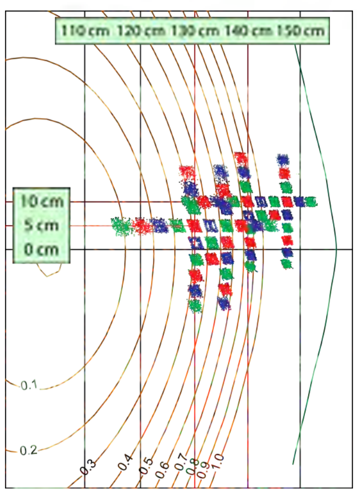

High-k Microwave Scattering

Detect radiation scattered from collimated 280GHz (~1mm) microwave beam

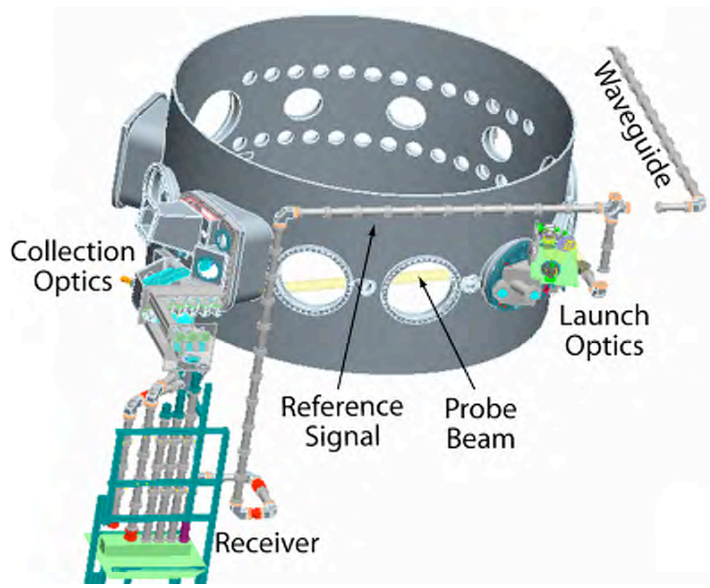

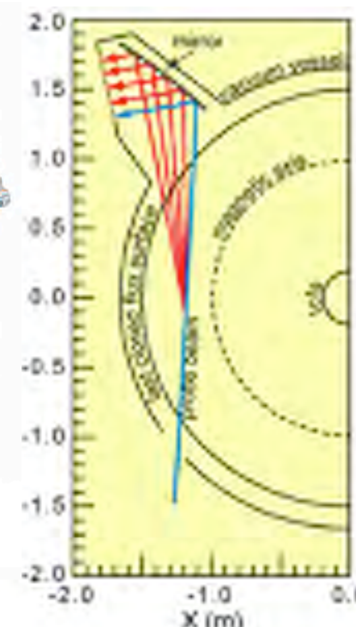

For fluctuations with wavevector $\boldsymbol{k_P}$, frequency ω_P

$\boldsymbol{k_S} = \boldsymbol{k_0} + \boldsymbol{k_P}$ and $\omega_S = \omega_0 \pm \omega_P$

D. Smith et al., RSI **81** (2010) 10D717

Heating Electrons with HHFW Power Drives Short-Wavelength Turbulence in Plasma Core

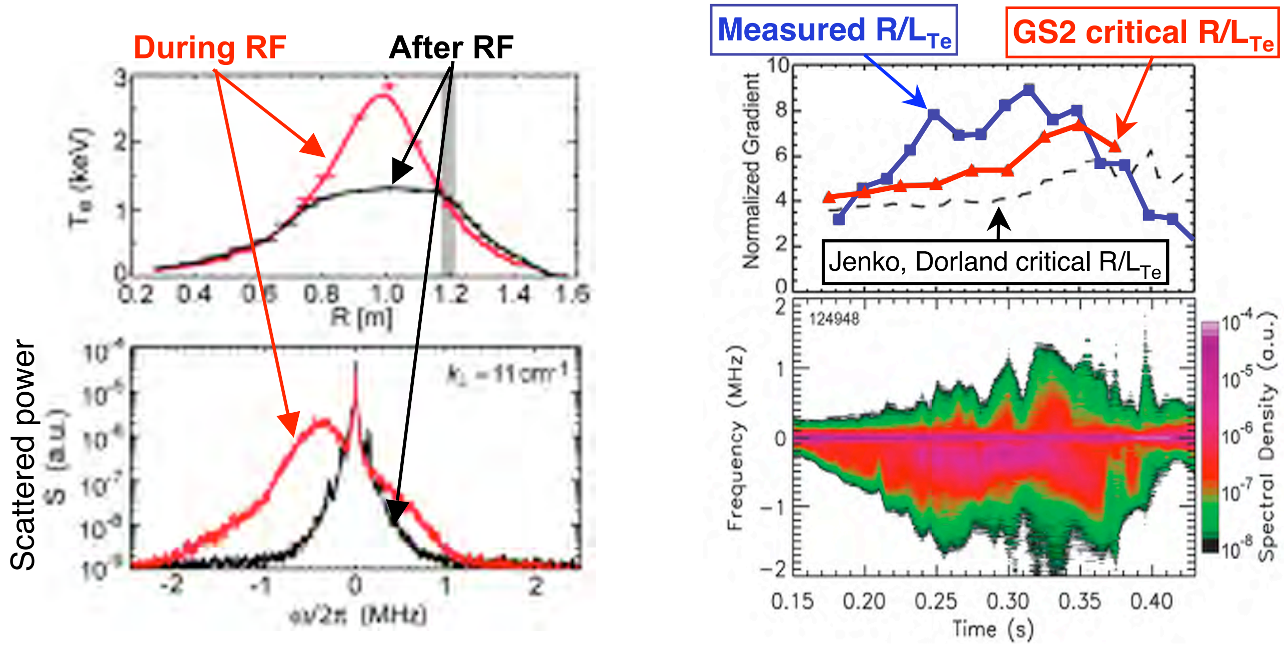

- Detected fluctuations in range $k_\perp\rho_e = 0.1 – 0.4$ ($k_\perp\rho_s = 8 – 16$) propagate in electron diamagnetic drift direction
  - Rules out Ion Temperature Gradient mode ($k_\perp\rho_s \sim 1$) as source of turbulence
  - Reasonable agreement with linear gyrokinetic code (GS2) in threshold for destabilization of **Electron Temperature Gradient** (**ETG**) modes
- Measured R/L_{Te} *does exceed* threshold ⇒ ETG-induced transport is not "stiff"

E. Mazzucato et al., *NF* ***49*** *(2009) 055001*

Reduction in High-k Turbulence Consistent With Reduced Electron Heat Transport in Outer Plasma

- Compare discharges **with** and **without** lithium applied
  - Discharges with lithium have higher global confinement
- Fluctuation spectra measured with microwave scattering

Measured density fluctuation vs. $k_\perp \rho_s$

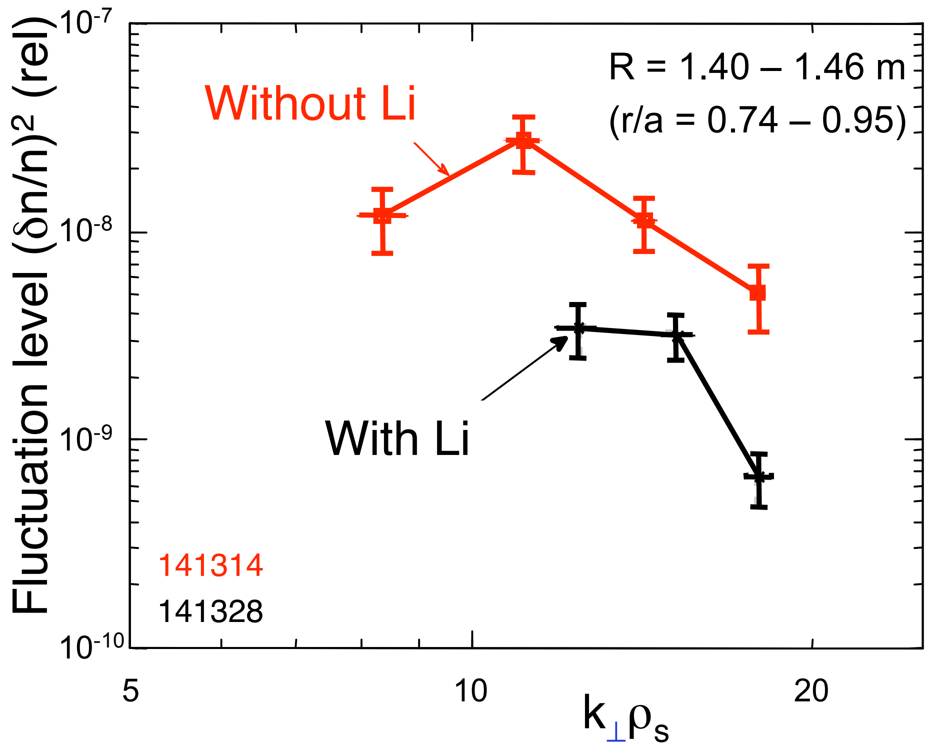

χ_e profile (TRANSP)

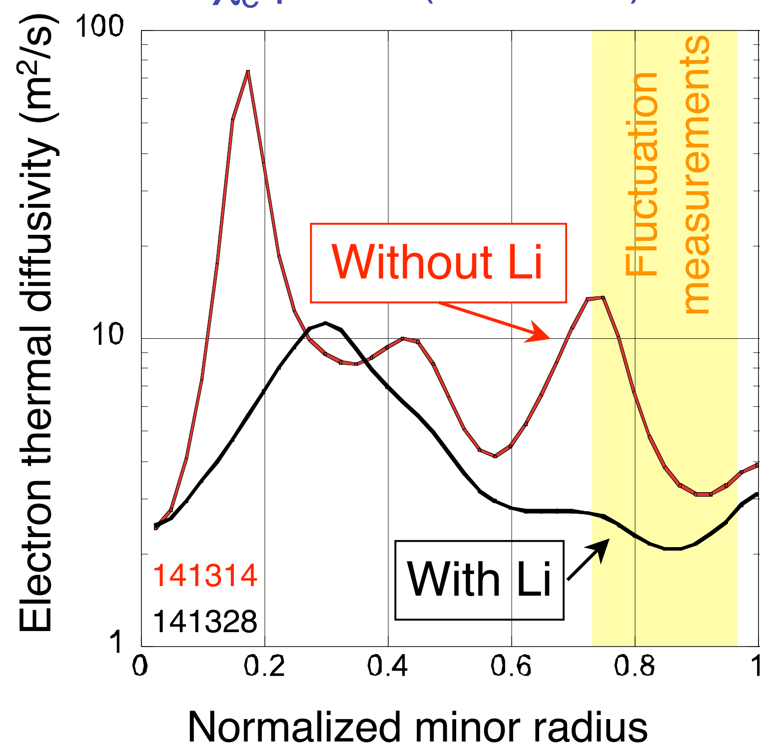

ρ_s = ion sound-speed gyro-radius = $\sqrt{[\gamma m_i (kT_e)/Z_i]}/eB$

Y. Ren et al., *PoP* ***19*** *(2012) 056125*

Electron Gyro-Scale Fluctuations Suppressed by Negative Magnetic Shear in Plasma Core

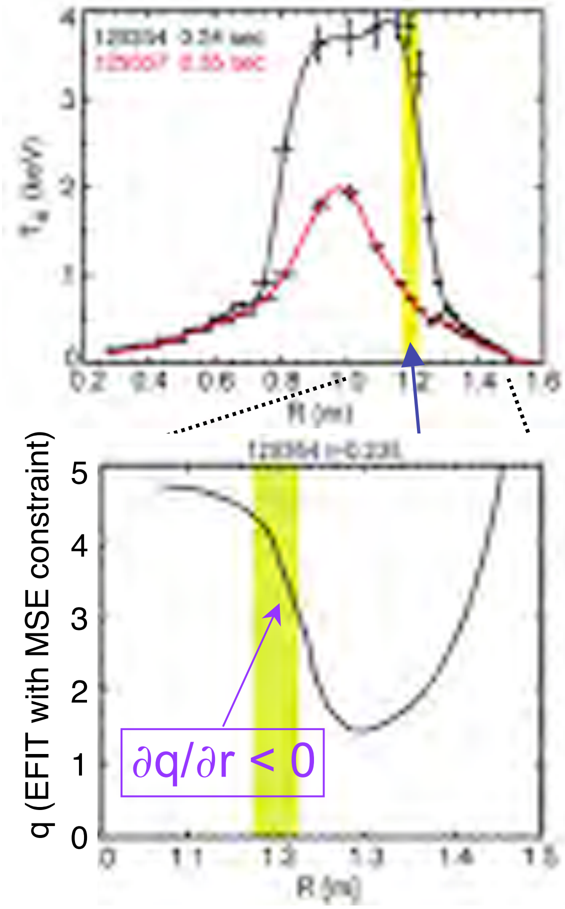

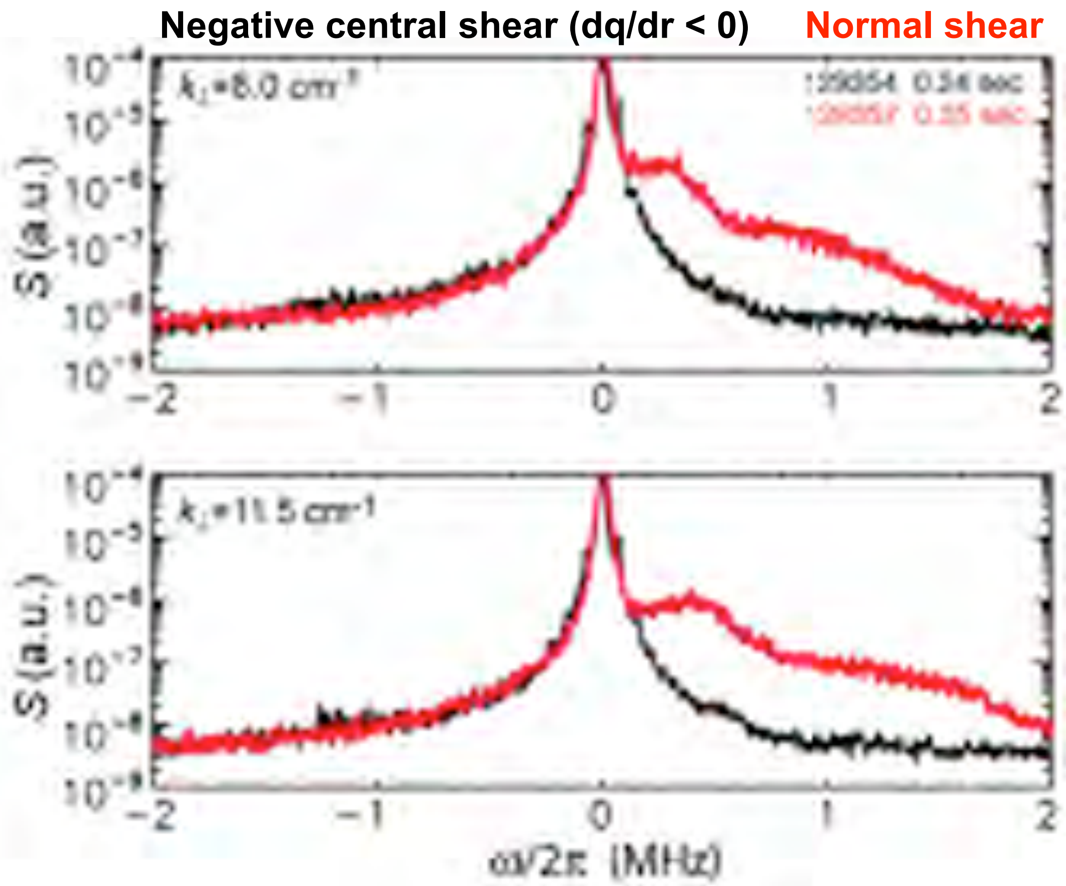

- Suppression of Electron Temperature Gradient (ETG) driven turbulence by shear-reversal had been predicted (F. Jenko & W. Dorland, PRL 2002)
- Shear-reversed q-profile is compatible with bootstrap driven current

H. Yuh et al., PoP ***16*** *(2009) 056120*

Strong Confinement Dependence on Collisionality Reproduced in Micro-Tearing Turbulence Simulations

Experiment

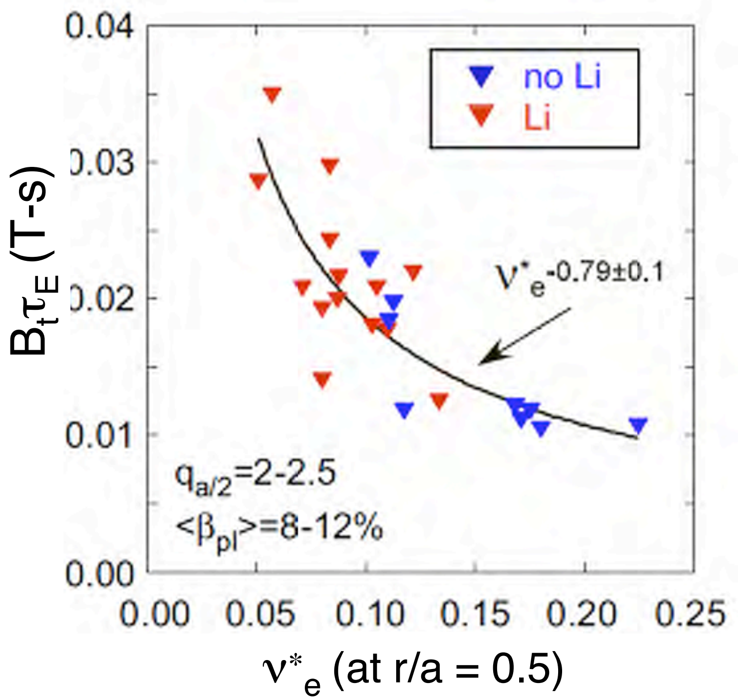

- Lithium has enabled NSTX to achieve lower collisionality
- Strong increase in τ_E as ν^*_e decreases ($\tau_E \propto \chi_e^{-1}$)

Simulations of Micro-Tearing

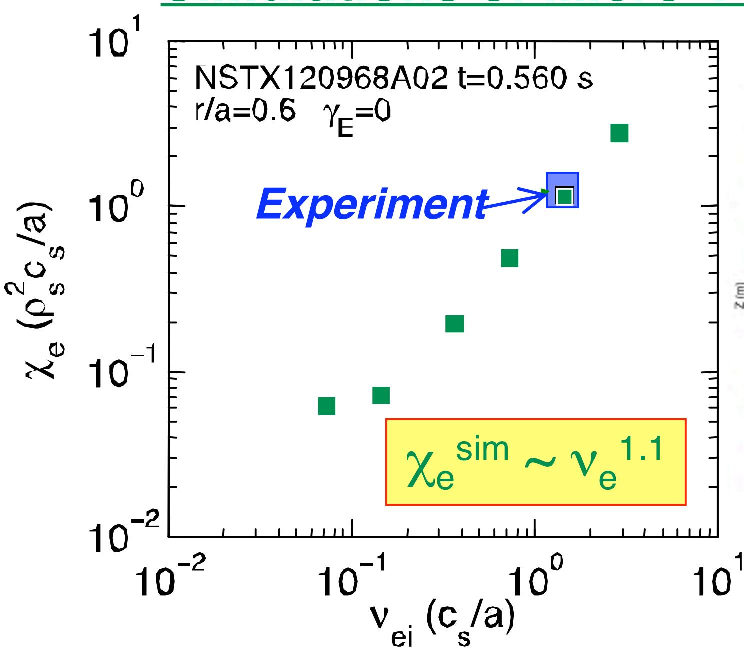

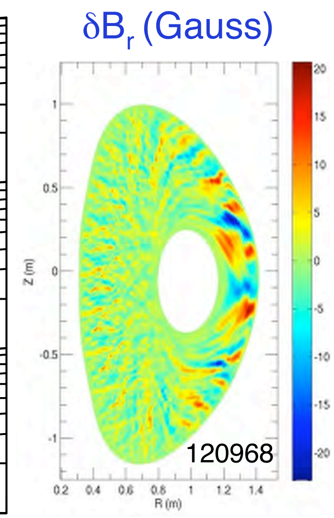

- Follow mode evolution to "steady" state
- Collisionality varied from experiment
- Predicted χ_e and scaling consistent with experiment ($\Omega\tau_E \sim B_t\tau_E \sim \nu^*_e{}^{-0.8}$)
- Transport dominated by magnetic "flutter"

 S. Kaye et al., IAEA FEC 2012, to be published W. Guttenfelder, et al., PRL **106**, 155004 (2011)

NSTX Accesses Fast-Ion Phase-Space Regime Overlapping With and Extending Beyond ITER

- Energetic ions from NBI heating in NSTX mimic alpha-particles in ITER
- Energetic ions interact with Alfvén waves and excite *toroidal eigenmodes*
- When many modes grow they can form an "avalanche instability" which modifies the particle orbits and can eject some ions

Frequency spectra of magnetic fluctuations

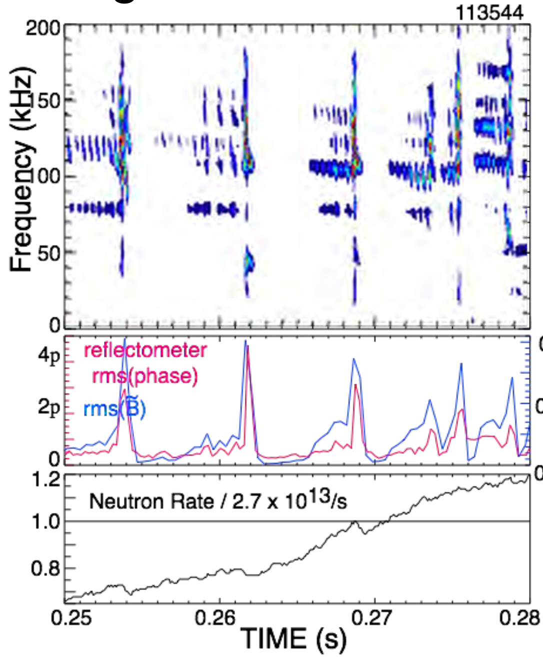

Density of fast ions 30–65 keV measured spectroscopically

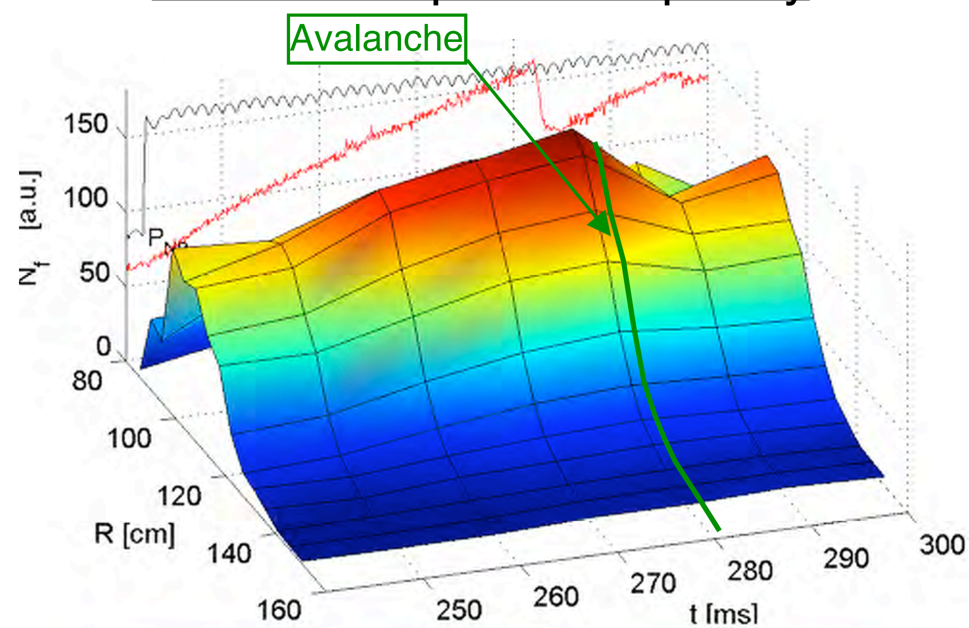

M. Podestà et al., *PoP* ***16*** *(2009) 056104*

Low Frequency MHD Instabilities Can Also Redistribute Fast Ions

- Initial modes are kink-like, global instabilities with frequencies typically a few kHz
  - Primarily n = 1, weaker n = 2 present
- Add 3-D perturbed field to 2-D equilibrium field and follow orbits of an ensemble of test particles by integration of Lorentz force (SPIRAL code)
- Energetic ions are redistributed
  - Outward radially
  - Towards $V_{||}/V = 1$
- This redistribution can then affect stability of other modes: *AE, RWMs
  - CAE activity observed *after* onset of low frequency MHD
- CAEs are possible cause of enhanced core electron transport
  - Resonant with electron orbit frequencies

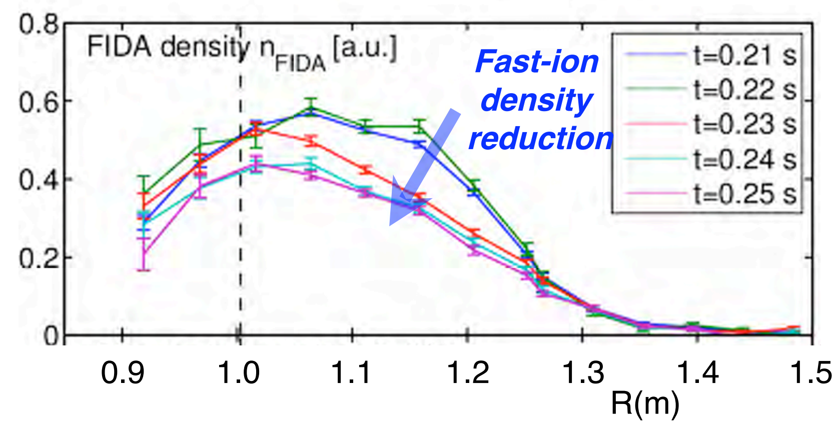

Calculated change in fast-ion distribution due to kink mode

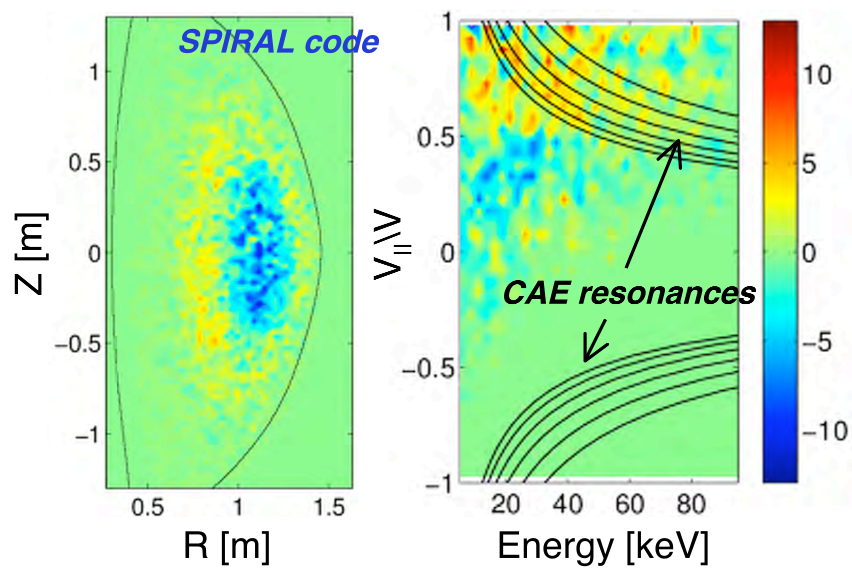

A. Bortolon to be submitted to PoP 2012

TAE Avalanches Lead to Broadening of the Beam Driven Current Profile

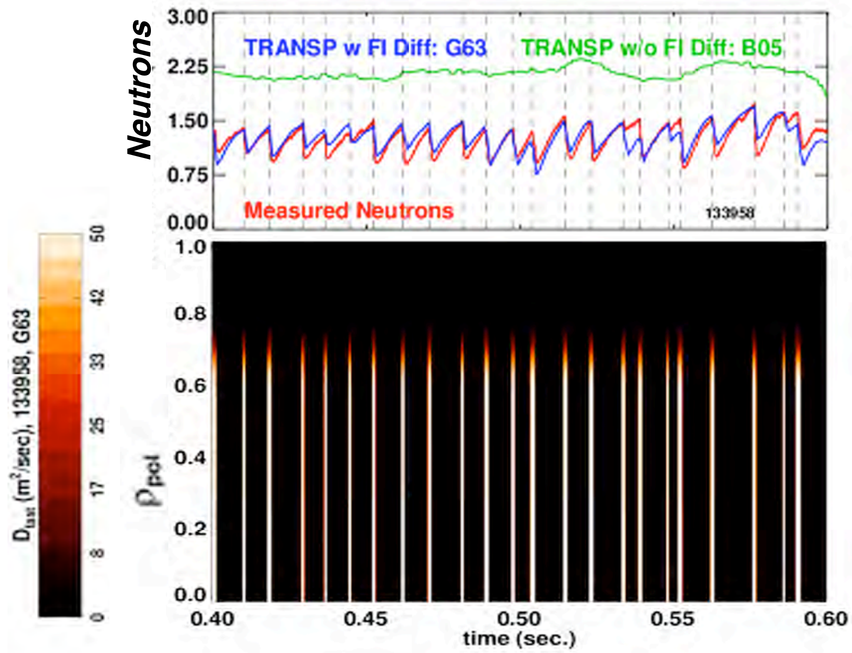

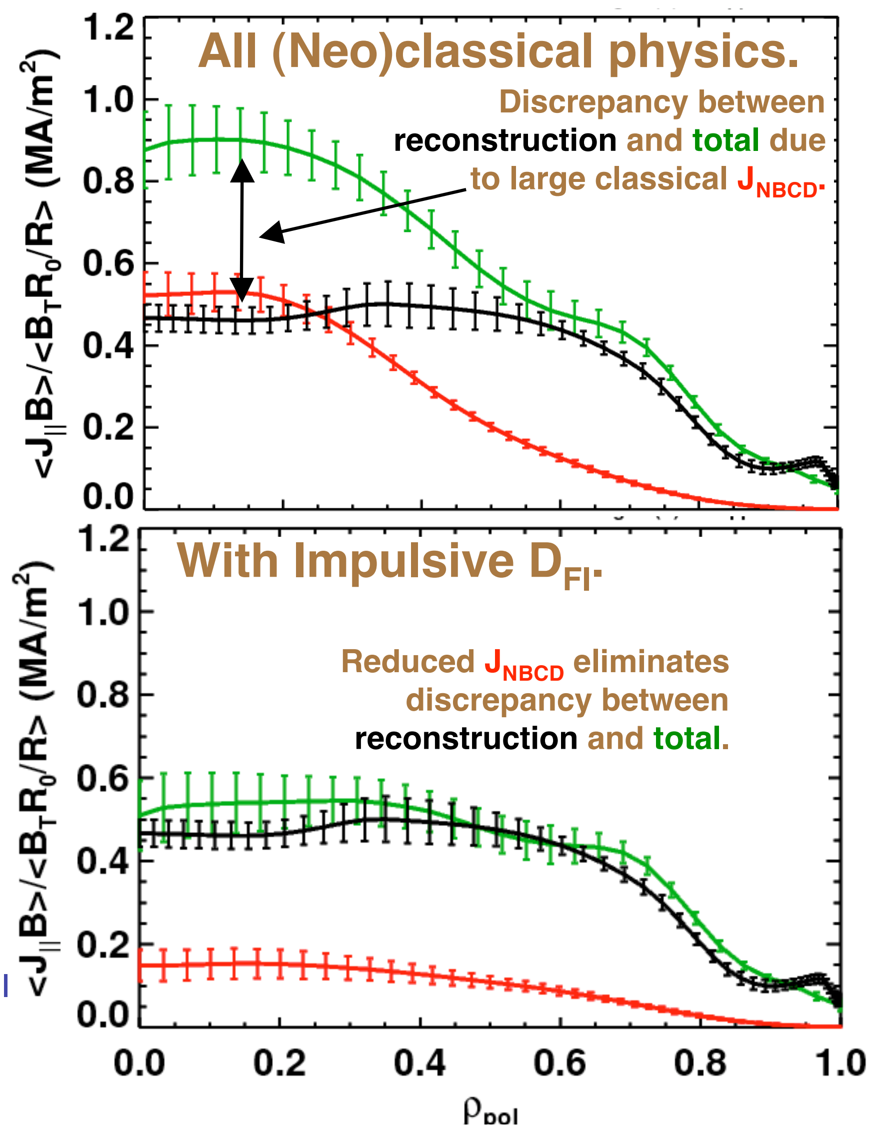

- Repetitive bursts in 20 – 100 kHz range
- Model using spatially and temporally localized fast-ion diffusivity $D_{FI}(\psi,t)$
  - Use DD neutron dynamics to determine D_{FI}
  - Modeled current profile then matches that inferred from magnetic data

S. Gerhardt et al., *NF* ***51*** *(2011) 033004*

Generating and Sustaining the Toroidal Plasma Current in the ST

- There is very little room for a central solenoid winding in the ST
  - Flux swing scales with the square of solenoid radius
  - Protecting the insulation from neutron damage would be very challenging
  - Schemes have been proposed to use iron cores or removable solenoids
- The bootstrap current can provide a large fraction of the toroidal plasma current in the ST
  - Scales as $\sqrt{\varepsilon}\beta_P$
- High-energy NBI can also drive significant current
  - Requires an initial toroidal current ~1MA to confine the ions
- However, techniques are needed to initiate current and to control its profile to maintain optimum MHD stability

We will now discuss methods being investigated in NSTX and MAST

- *Many other STs are also actively exploring current drive schemes*

NSTX Developing Coaxial Helicity Injection (CHI) for Non-Inductive Initiation of Toroidal Plasma Current

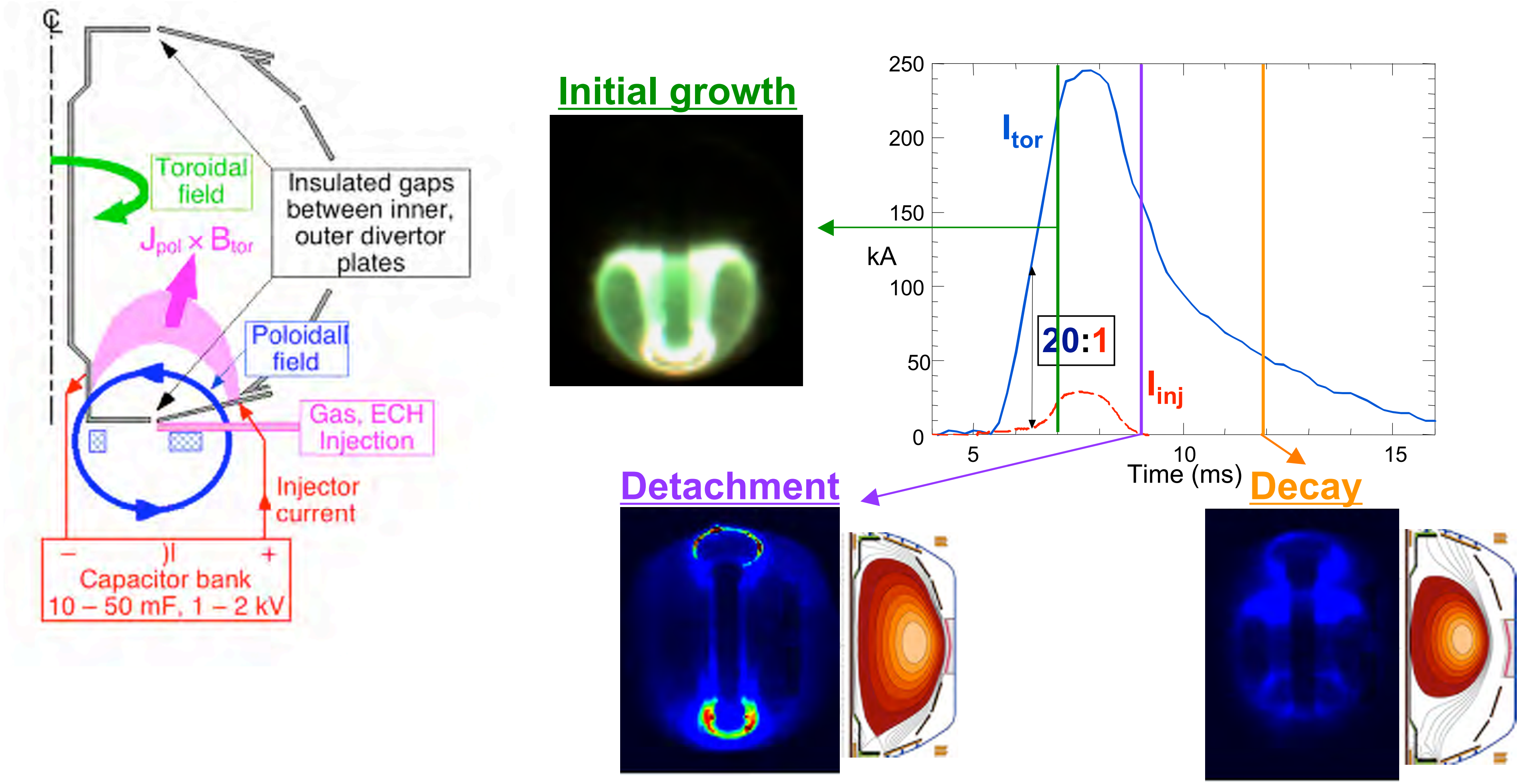

- After $I_{CHI} \to 0$, toroidal plasma current flows on closed flux surfaces
- Without additional heating and current drive, current decays resistively

R. Raman et al., *NF* ***49*** *(2009) 055014*

CHI Produced Substantial Increases in Plasma Current for Same Applied Inductive Flux

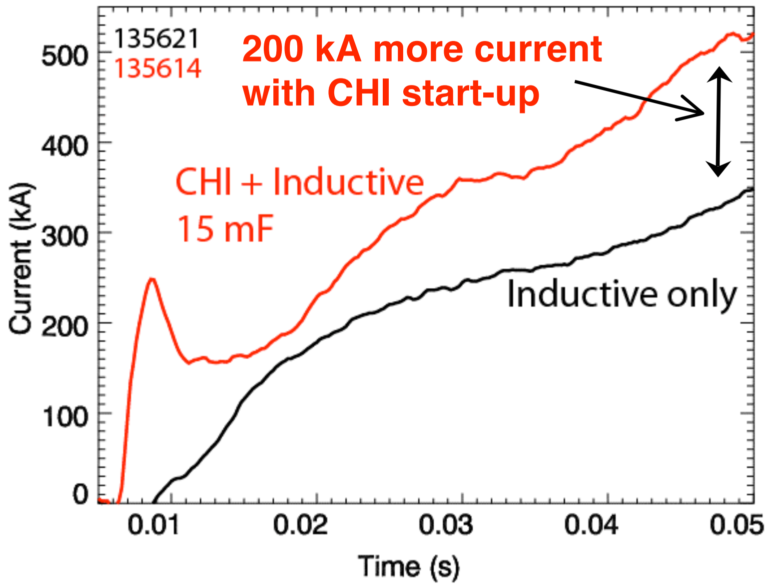

Electron temperature profile after CHI

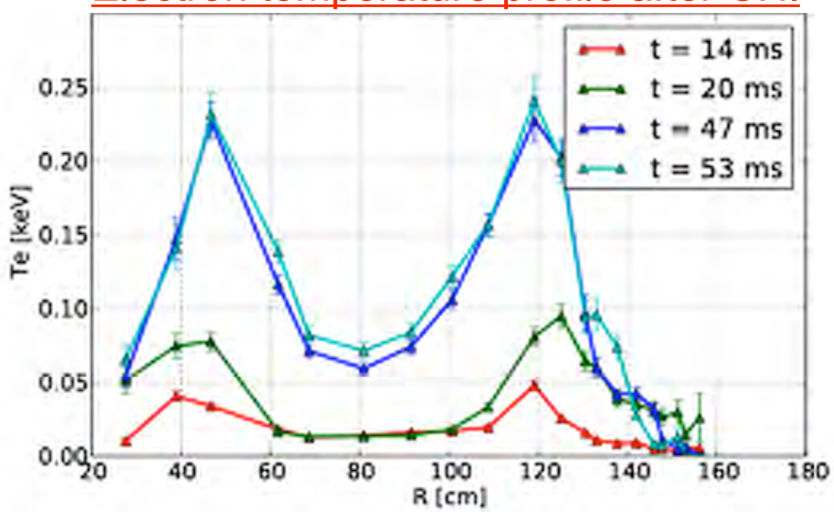

- Lithium coating of lower divertor (electrodes) improved CHI initiation
  - Reduced radiation by carbon and oxygen impurities
- Discharges compared had same waveform of solenoid current
- Reached 1MA using 40% less flux than induction-only case
  - Hollow T_e maintained during current ramp following CHI
  - Higher average T_e reduced resistive flux consumption
  - Low normalized internal inductance $l_i \approx 0.35$
  - Aids achieving high elongation

B. Nelson et al., *NF* ***51*** *(2011) 063008*

Evidence for Current Drive by HHFW by Comparing Co- and Counter- CD Phasing

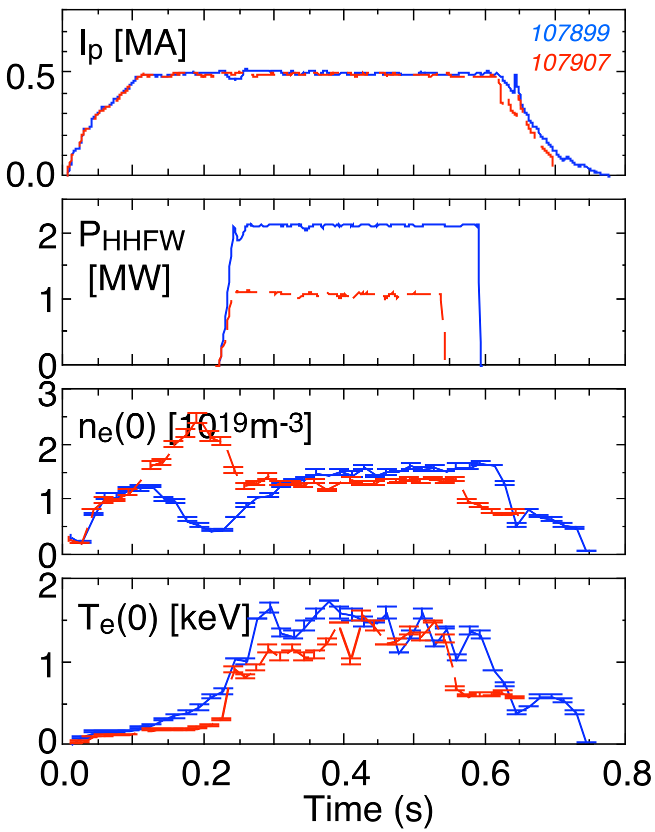

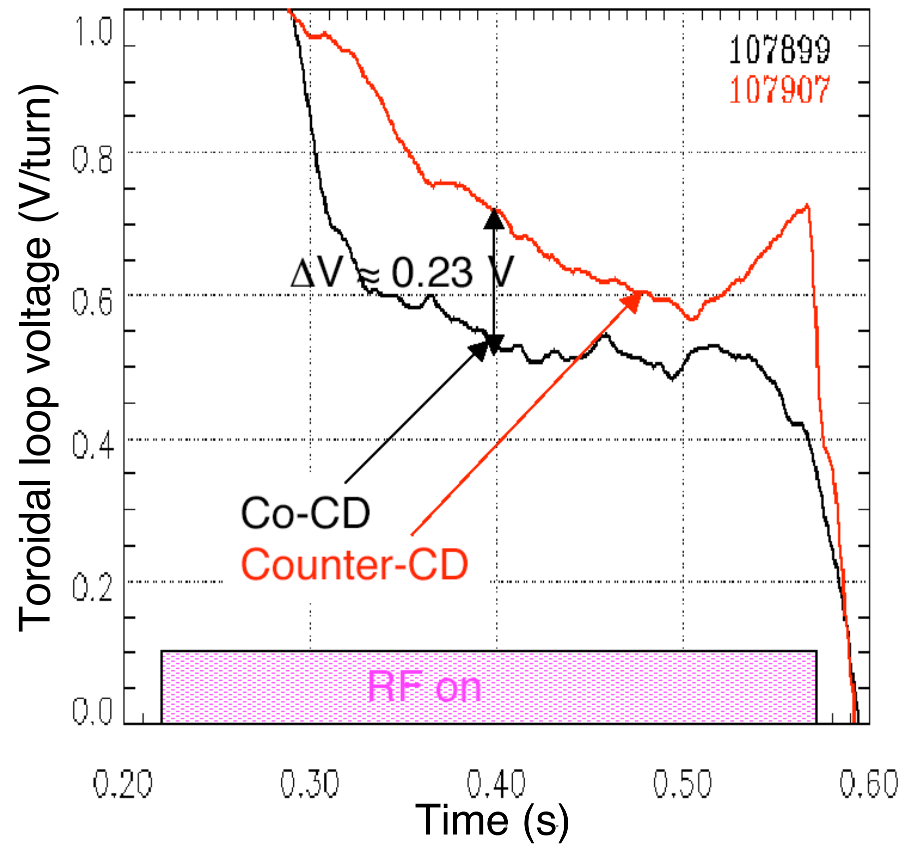

- Wavenumber $k_T \approx \pm 7m^{-1}$ – phase velocity matches ~2keV electrons
- Inductive loop voltage controled by feedback to maintain plasma current
- Difference in voltage required implies 150kA driven by HHFW
- Codes modeling wave interaction calculate 90 – 230 kA driven by waves

MAST Used Waves in Electron Cyclotron Frequency Range to Drive Current

MAST

- Electron cyclotron frequency: $f_{ce} = eB/2\pi m_e$ = 28GHz @ 1T
- O-mode waves only propagate *above* the electron plasma frequency: $f_{pe} = \sqrt{(n_e e^2/\varepsilon_0 m_e)}/2\pi$ = 28GHz @ 1×10^{19}m^{-3}
- ST plasma is typically "overdense" $\Rightarrow$ must rely on other wave modes
- The electrostatic **Electron Bernstein Wave** (EBW) can be generated by **Mode Conversion** in a plasma from externally launched e.m. waves

- MAST used a mirror with slanted grooves on its center column to change the polarization of waves launched from the outboard side
- The reflected waves (X-mode) convert to EBW in the plasma
- When EBW are absorbed on resonant electrons they can generate current

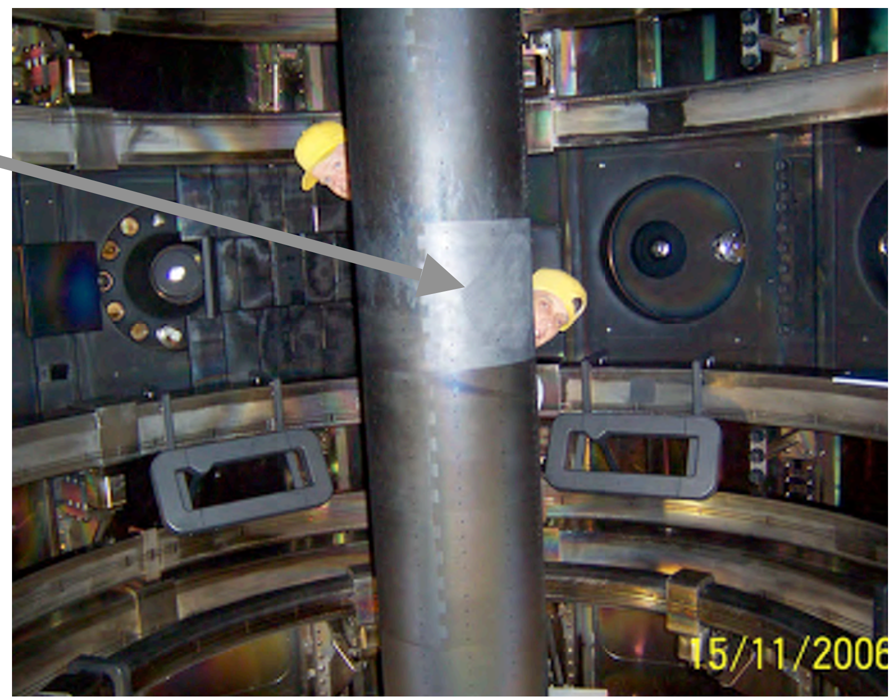

Courtesy of B. Lloyd and MAST group, CCFE, UK

100 kW of 28GHz RF Power Generated 17kA Plasma Current by EBW CD in MAST

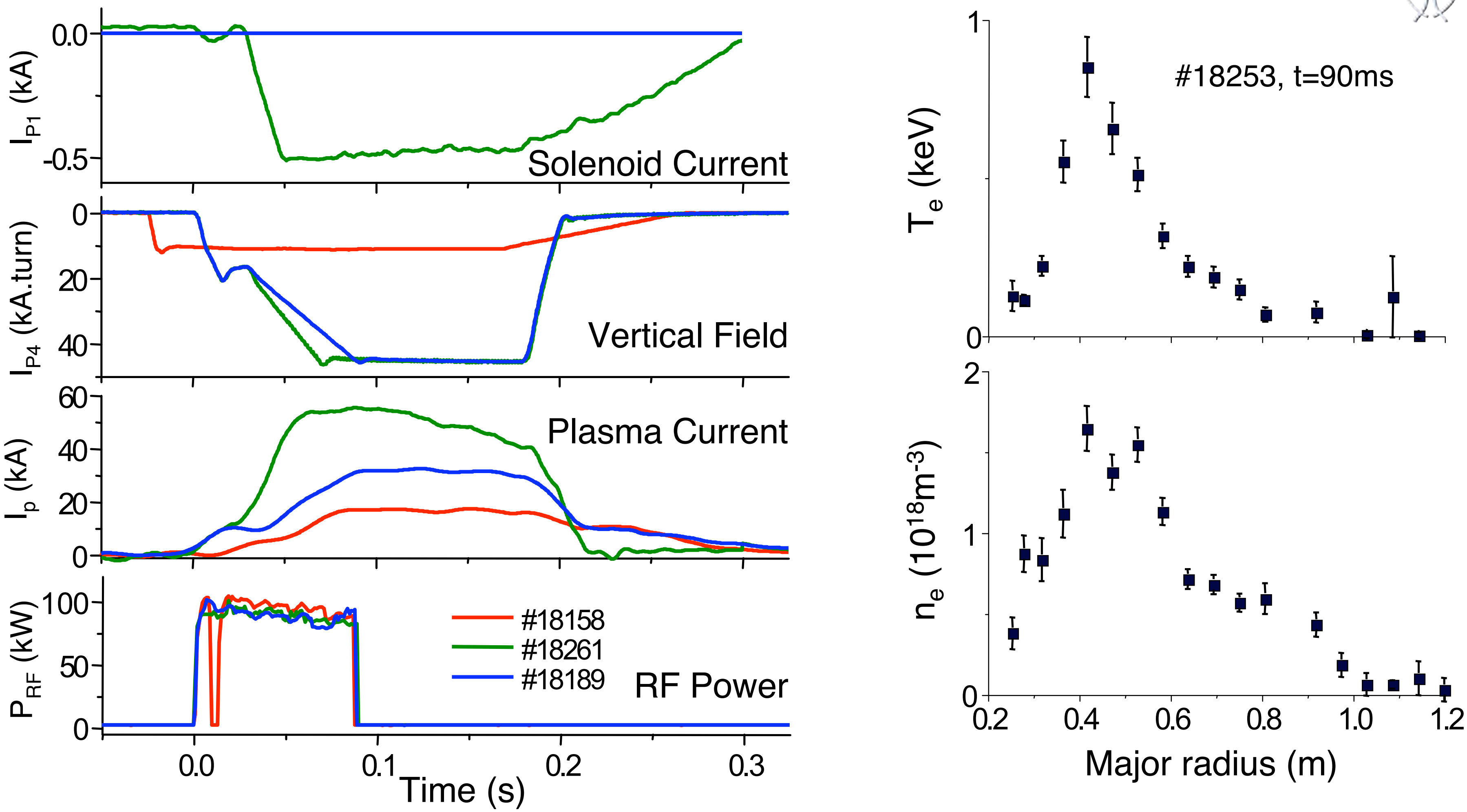

- EBW-driven current augmented by flux from Vertical Field and Solenoid
- Temperature and density peak at electron cyclotron resonance layer

V. Shevchenko et al., *NF* **50** (2010) 022004

The ST Is Making Good Progress Toward a FNSF While Contributing to the Physics Basis of ITER

- Ability of the ST to achieve high β now well established
- Advanced plasma stabilization methods and diagnostics being applied to improve performance
- Provides a unique opportunity to study transport and turbulence
- Investigating fast-ion instabilities relevant to ITER
- Developing innovative solutions to heat-flux management
- Developing non-inductive startup and sustainment schemes
- **NSTX** is currently undertaking a major refit to install additional NBI heating and upgrade its coils
  - Double its NBI power and magnetic field and extend its pulse-length
- **MAST** will soon install its Super-X divertor and upgrade its heating